Quaternary Science Reviews 141 (2016) 65–84

Contents lists available at ScienceDirect

Quaternary Science Reviews

journal homepage: www.elsevier.com/locate/quascirev

Strontium isotope investigation of ungulate movement patterns on the Pleistocene Paleo-Agulhas Plain of the Greater Cape Floristic Region, South Africa

Sandi R. Copeland [a, b, *], Hayley C. Cawthra [c, d], Erich C. Fisher [d, e, f], Julia A. Lee-Thorp [g], Richard M. Cowling [d], Petrus J. le Roux [h], Jamie Hodgkins [i], Curtis W. Marean [d, e]

[a] Environmental Stewardship Group, Los Alamos National Laboratory, MS J978, Los Alamos, NM 87545, USA
[b] Department of Anthropology, University of Colorado Boulder, Campus Box 233 UCB, Boulder, CO 80309-0233, USA
[c] Geophysics Competency, Council for Geoscience, PO Box 572, Bellville, 7535, South Africa
[d] Centre for Coastal Palaeoscience, Nelson Mandela Metropolitan University, PO Box 77000, Port Elizabeth, 6031, South Africa
[e] Institute of Human Origins, School of Human Evolution and Social Change, Arizona State University, Tempe, AZ 85287-2402, USA
[f] Evolutionary Studies Institute, University of the Witwatersrand, Private Bag 3, Wits 2050, South Africa
[g] Research Laboratory for Archaeology, University of Oxford, Oxford, OX1 3QY, UK
[h] Department of Geological Sciences, University of Cape Town, South Africa
[i] Department of Anthropology, University of Colorado Denver, P.O. Box 173364, Denver, CO 80217-3364, USA

ARTICLE INFO

Article history:
Received 29 September 2015
Received in revised form
15 March 2016
Accepted 3 April 2016
Available online 16 April 2016

Keywords:
Strontium isotopes
Middle Stone Age
South Africa
GIS model
Archaeology
Ungulate paleoecology
Migration
Fossils
Greater Cape Floristic Region
Intra-tooth

ABSTRACT

Middle Stone Age sites located within the Greater Cape Floristic Region on the South African southern coast have material culture with early evidence for key modern human behaviors such as projectile weaponry, large animal hunting, and symbolic behavior. In order to interpret how and why these changes evolved, it is necessary to understand their ecological context as it has direct relevance to foraging behavior. During periods of lowered sea level, a largely flat and vast expanse of land existed south of the modern coastline, but it is now submerged by higher sea levels. This exposed area, the Paleo-Agulhas Plain, likely created an ecological context unlike anything in the region today, as evidenced by fossil assemblages dominated by migratory ungulates. One hypothesis is that the Paleo-Agulhas Plain supported a migration ecosystem of large grazers driven by summer rainfall, producing palatable forage during summer in the east, and winter rainfall, producing palatable forage during winter in the west. Alternatively, ungulates may have been moving from the coastal plain in the south to the interior north of the Cape Fold Mountains, as observed for elephants in historic times.

In this study, we assess ungulate movement patterns with inter- and intra-tooth enamel samples for strontium isotopes in fossil fauna from Pinnacle Point sites PP13B and PP30. To accomplish our goals we created a bioavailable $^{87}Sr/^{86}Sr$ isoscape for the region by collecting plants at 171 sampling sites and developing a geospatial model. The strontium isotope results indicate that ungulates spent most of their time on the Paleo-Agulhas Plain and avoided dissected plain, foothill, and mountain habitats located more than about 15 km north of the modern coastline. The results clearly exclude a north-south (coastal-interior) movement or migration pattern, and cannot falsify the east-west movements hypothesized in the south coast migration ecosystem hypothesis.

© 2016 Elsevier Ltd. All rights reserved.

1. Introduction

A series of South African Middle Stone Age (MSA) sites dating from ~160 to 50 ka provide evidence that has revised our understanding of the timing and pace of behaviors considered indicative of modern humans. Many of these sites are on the coast of the Greater Cape Floristic Region (GCFR) (Fig. 1), an area with Mediterranean climate and unique vegetation that is a plant biodiversity hotspot and center of endemism (Allsopp et al., 2014), but which is currently depauperate in large ungulates. The locality of our study

* Corresponding author.Environmental Stewardship Group, Los Alamos National Laboratory, MS J978, Los Alamos, NM 87545, USA.
E-mail address: sandicopeland@gmail.com (S.R. Copeland).

http://dx.doi.org/10.1016/j.quascirev.2016.04.002
0277-3791/© 2016 Elsevier Ltd. All rights reserved.

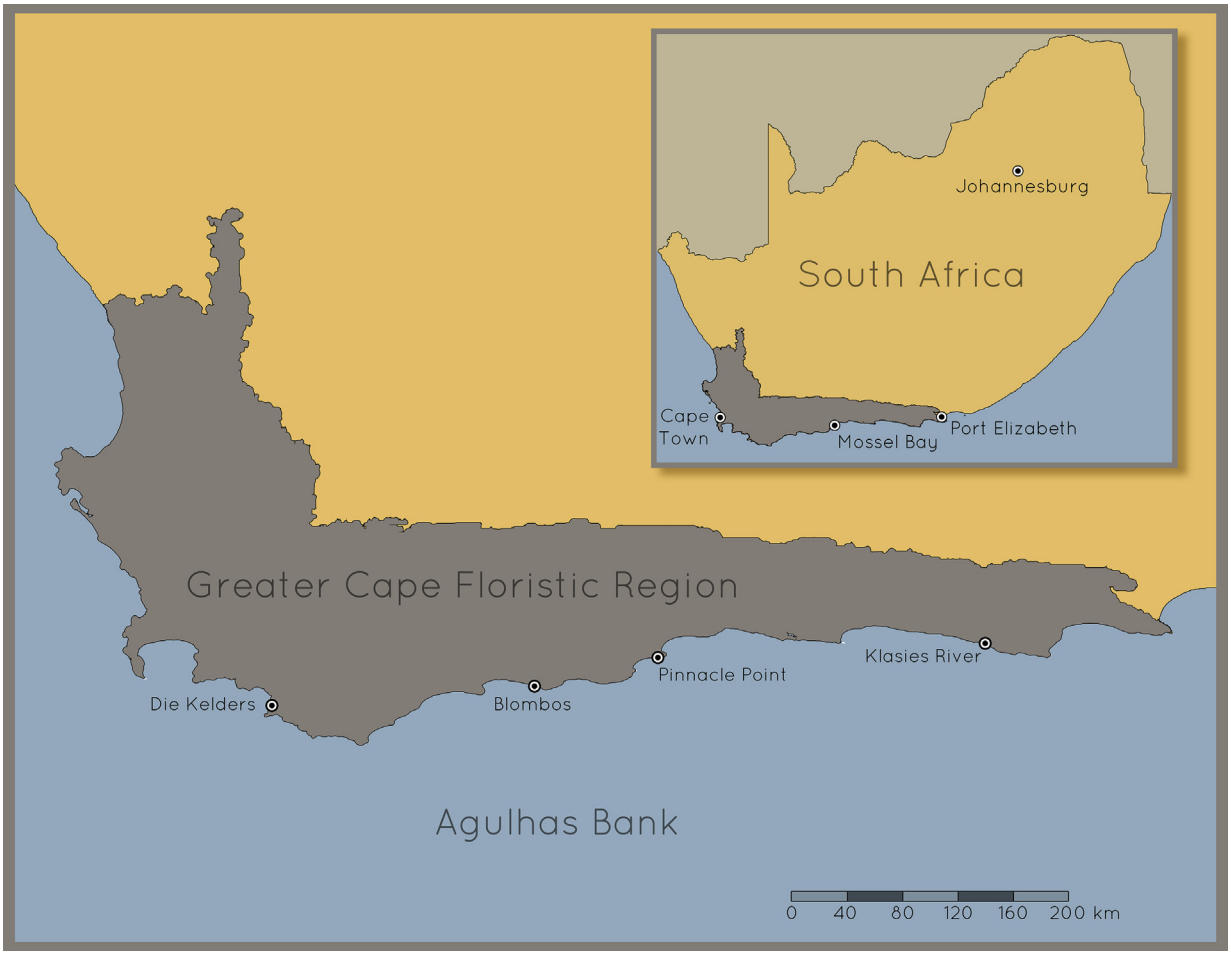


Fig. 1. Map of southern Africa showing the extent of the Greater Cape Floristic Region with important cities (inset) and Middle Stone Age/Late Stone Age archaeological sites.

is Pinnacle Point, which is within the GCFR (Marean et al., 2014) and contains sites with the earliest evidence for stone tool microlithic technology ~71 ka (Brown et al., 2012), heat-treated stone tool production ~160 ka (Brown et al., 2009), and early evidence for humans using coastal resources ~160 ka (Marean, 2014; Marean et al., 2007). Genetic and fossil evidence suggest that the modern human lineage appears by at least ~200–160 ka (Clark et al., 2003; Gonder et al., 2007; McDougall et al., 2005), and of the handful of sites in Africa that are numerically dated to this time interval, only two are in South Africa (Border Cave and Pinnacle Point 13B) and one of these is in the GCFR (Pinnacle Point 13B) (Marean et al., 2007). It has been hypothesized (Marean, 2011, 2010) that the origin lineage of the indigenous inhabitants of the southern African sub-region, identified by genetic evidence (Henn et al., 2011; Pickrell et al., 2012; Schlebusch et al., 2012), found refuge along the southern shorelines during the long glacial cycle of Marine Isotope Stage (MIS) 6 (~195–125 ka) (Petit et al., 1999). For these reasons there is an ongoing multi-disciplinary effort to develop a detailed reconstruction of the paleoecological context of this region during the origins of modern humans (Franklin et al., 2015; Marean et al., 2014, 2015).

Klein (1983) noted that the faunal changes in the GCFR from the Pleistocene to the Holocene were greater than in any other African region with the possible exception of the Maghreb. Archaeological sequences dating to the Holocene —when the current sea levels and patterns of climate were rather stable and similar to modern — document a terrestrial fauna dominated by small-bodied residential species such as grysbok, hyrax, dune mole rats, and tortoises (Marean et al., 2014). In contrast, the Pleistocene MSA and Later Stone Age (LSA) sequences found along the South African coast were dominated by large and medium-sized ungulates (both extinct and extant) that are typical of open-habitat migratory ecosystems (Klein, 1983). An early microlithic stone tool technology found at Pinnacle Point is further hypothesized to have been a component of projectile weapons designed to hunt large mammals safely and effectively (Brown et al., 2012). Open-habitat species that were present in the Pinnacle Point MSA levels (Rector and Reed, 2010) include black wildebeest (*Connochaetes gnou*), hartebeest (*Alcelaphus buselaphus*), springbok (*Antidorcas marsupialis*), zebra (*Equus* cf. *quagga*), and the extinct giant buffalo (*Syncerus antiquus*). Prior to fencing and habitat destruction, some of these species formed migratory associations of millions of animals in the interior well north of the south coast in the South African Highveld and Karoo that did not penetrate into the GCFR (Cronwright-Schreiner, 1925; Estes, 1991).

The dramatic faunal change between glacial and interglacial climates may seem surprising given that the GCFR was subject to rather muted climatic change through the Pleistocene (Chase and Meadows, 2007; Marean et al., 2014). Off the coast of the GCFR is the gradually descending and low-relief Agulhas bank, and during periods of lowered sea level varying portions of this landmass were exposed (Van Andel, 1989). A computer model of the changing character of this “Paleo-Agulhas Plain” shows that it was relatively flat, and during peak sea level regressions exposed about

80,000 km^2 of land (Fig. 2) – equivalent to the size of Ireland (Fisher et al., 2010). The plain is hypothesized to have been a refuge for humans during glacial phases (Compton, 2011). Marine geophysics studies provide further details and document the presence of broad floodplains (Cawthra et al., 2015). Thus, while changes in climate may have been relatively subtle between the Pleistocene and Holocene, changes in the landmass of the GCFR were huge and probably drove ecological change in the region (Marean et al., 2014). Furthermore, the character of the coastal foreland differed both geomorphologically and edaphically. The modern/Holocene coastal foreland is composed of highly dissected Paleogene rocks, whereas the variably exposed Paleo-Agulhas Plain of the Pleistocene was dominated by Cretaceous mudstones proximally and marine sediments distally (Cawthra et al., 2015). The soils derived from Paleo-Agulhas Plain substrata would have been considerably more fertile than those derived from the ancient rocks of its hinterland.

The current GCFR does not support the large grazers that were common in the Pleistocene, so what differences might account for this? Within the GCFR (Fig. 1) there is a gradient of increasing summer rain from west to east along the south coast. West of Cape Agulhas is the winter rainfall zone in which more than 66% of mean annual precipitation falls between April–September (Chase and Meadows, 2007). Between Cape Agulhas and Mossel Bay, rainfall is bimodal with peaks in spring and autumn and with reliable winter but unreliable summer rain. East of Mossel Bay, rainfall is similarly bimodal but with increasingly reliable summer component (Bradshaw and Cowling, 2014). Further east and north, beyond the GCFR, is the summer rainfall zone (Schulze, 1972). Carbon and oxygen isotope evidence in speleothems from Pinnacle Point (Bar-Matthews et al., 2010) and carbon isotope evidence from Nelson Bay Cave fauna (Sealy, 1996) suggest that this east-west rainfall gradient was a persistent feature during the Late Pleistocene. Furthermore, the presence of the GCFR itself indicates the persistence of this flora that is typically low in grasses over great time depth.

During lower sea levels, the large, flat Paleo-Agulhas Plain may have provided the environmental conditions for a greater grassy component on the landscape. The grasses could have occurred in extensive grasslands, but it is also possible that grasses grew as a component of grassy shrublands, or that grasses were concentrated in localized habitats such as seasonally waterlogged areas, as is

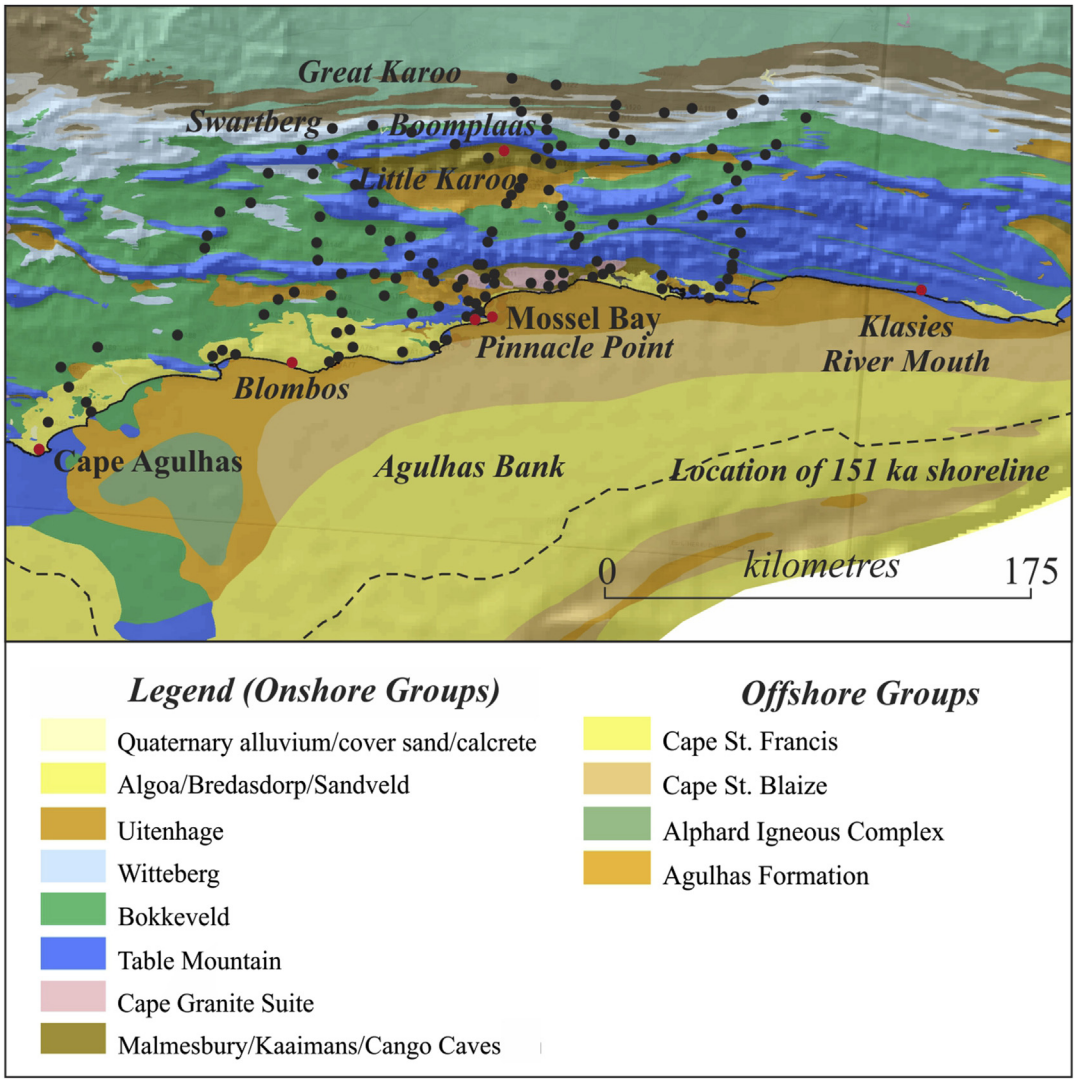


Fig. 2. Map of the South African Coast showing bedrock geology, the modern coastline (solid black line), and the extent of the 151 ka shoreline (the time of PP30 fossil accumulation, dashed black line). Black dots show sampling localities at which plants were collected for biologically available $^{87}Sr/^{86}Sr$. Red dots indicate modern cities and archaeological sites. (For interpretation of the references to color in this figure legend, the reader is referred to the web version of this article.)

found in the eastern GCFR today (Cowling and Potts, 2015). Bimodal rains falling on the easterly portion of the GCFR may have produced fresh grass during the warm season whereas the winter rains in the west produced expanses of fresh grass during the winter. A speleothem record dating from 90 to 53 ka has been interpreted as indicating an increase in the amount or proportion of summer rain during MIS 4 in the Pinnacle Point region (Bar-Matthews et al., 2010). Such changes in the distribution of summer and winter rain in the past may have had significant impacts on the suitability of the region for an east-west migratory system.

These rainfall conditions were hypothesized to provide the push and pull for a classic migration ecosystem on the Paleo-Agulhas Plain in the Pleistocene whereby animals moved east and then west to take advantage of summer and winter rains and green grass, respectively (Marean, 2010; Marean et al., 2014). The mortality patterns of fossil specimens of the blue antelope *Hippotragus leucophaeus* from sites along the south coast are consistent with an east-west migration (Faith and Thompson, 2013). An alternative hypothesis is that animals moved along a north-south axis, migrating from the coastal plains, through mountain passes of the Outeniqua Mountains, and into the Little Karoo intermontane basin. Historical observations that elephants followed such a path (Skead, 2011) are consistent with this hypothesis. The rapid rise of sea levels in the early Holocene submerged the Paleo-Agulhas Plain, and this may have been responsible for the regional extinction of a variety of ungulates at the Pleistocene/Holocene boundary (Marean, 2010; Marean et al., 2014).

In this study, we investigate animal movement patterns through the comparison of strontium ($^{87}Sr/^{86}Sr$) isotopes serially measured from fossil mammal teeth from the Pinnacle Point sites PP13B and PP30. Since the distribution of bioavailable $^{87}Sr/^{86}Sr$ across the GCFR has not been previously well documented, we develop an empirically grounded and robust strontium isoscape that includes a predictive geospatial model developed in GIS. We use the strontium isoscape to infer movement patterns of fossil animals from the sampled sites.

2. Background

2.1. Climate and environment

The south coast of South Africa lies at the confluence of two oceans (Atlantic and Indian) and two major oceanic systems - the cold Benguela Upwelling on the west coast and the warm Agulhas Current flowing down the east coast (Lutjeharms, 2006; Lutjeharms et al., 2001). There is an east-west gradient in plant carbon isotopes, with C_3 grasses giving way to proportionally more C_4 grass representation in the bimodal rainfall areas, and finally domination of C_4 grasses in the eastern summer rainfall areas (Cowling, 1983; Vogel et al., 1978). The present western, winter rainfall vegetation is not rich in grasses, but those that are present are mainly C_3. The vegetation in the eastern, summer rainfall zone is both richer in grasses and those present are largely C_4. Changes in the distribution of these rainfall and grass photosynthetic systems during portions of the late Pleistocene are reflected in the $\delta^{13}C$ of speleothems from Crevice Cave at Pinnacle Point (Bar-Matthews et al., 2010).

The GCFR is a Mediterranean vegetation that has one of the world's highest frequencies of endemic plants (69%) and is a region of megadiversity (Cowling and Lombard, 2002; Cowling et al., 2009; Goldblatt and Manning, 2002) and a globally-recognized biodiversity hotspot (Myers et al., 2000). The winter rainfall zone is thought to be the long-term stable core of the GCFR, with plant diversity and endemism declining from west to east (Cowling and Lombard, 2002).

The GCFR is composed of several biomes (Bergh et al., 2014). Fynbos forms the largest component, and is dominated by small-leafed evergreen shrubs and rushes (restios). It is typically found on nutrient-poor soils on leached quartzites and calcareous rocks, and fire is a key component of its regeneration. Thicket is found in areas protected from fire, and is dominated by evergreen shrubs and trees of tropical affinity; some forms comprise thicket clumps in a matrix of low, grassy shrubland (Vlok et al., 2003). Renosterveld, a grassy shrubland, is typically found on nutrient-rich soils (often on shales of the Bokkeveld Group). Renosterveld has been largely transformed for agriculture, and has been suggested as a potential vegetation type that supported large-bodied grazing species in pre-colonial times (Boshoff and Kerley, 2001; Boshoff et al., 2001). It is possible that the large numbers of grazing species in the Pleistocene could be explained at least partially by these species living in Renosterveld. However, if that were true, then prehistoric faunal assemblages from the Holocene should preserve these taxa, and they do not. Holocene faunal assemblages are overwhelmingly dominated by taxa typical of the current GCFR and lack the Pleistocene grazing communities (Marean et al., 2014).

2.2. Geology

Rocks of different types and ages are often distinct in strontium isotope ratios ($^{87}Sr/^{86}Sr$), therefore we provide a review of the geology of the region. The geological history of the South Coast spans the last 700 Myr from the Neoproterozoic sequences to recent unconsolidated beach and dune sediments flanking the modern shoreline. The oldest South Coast 'basement' rocks comprise the Malmesbury, Kaaimans, and Cango Caves Groups and the Cape Granite Suite (~650–510 Ma), related to Pan African orogenesis during the formation of Gondwana (Rozendaal et al., 1999; Johnson et al., 2006; Milani and de Wit, 2008). Overlying deposits of the Cape Supergroup form a 6–10 km thick siliciclastic sequence, divided into the Table Mountain, Bokkeveld and Witteberg Groups (Thamm and Johnson, 2006). The Cape Orogeny (~278–230 Ma; Newton et al., 2006) resulted in the formation of the Cape Fold Belt. The fragmentation of Gondwana in the South Coast region and the opening of the South Atlantic commenced in the Early Cretaceous (~136 Ma) (Martin and Hartnady, 1986). Compressional Cape Fold Belt faults were reactivated and the newly created accommodation space in basins was filled with clastic sediments of the Uitenhage Group (~145–130 Ma) (Paton et al., 2006). Offshore, arcuate normal faults bounded several graben and half graben structures that became the depocenters for terrigenous sediment sourced from the onshore areas (Broad et al., 2006; Tinker et al., 2008). Neogene and Quaternary aged Bredasdorp Group sediments are dominant along the southern coastal plain and include marine calcarenites (De Hoopvlei Formation), calcified aeolianites (Wankoe Formation), and aeolianites (Waenhuiskrans Formation) (Malan, 1990).

The southern coastal plain of South Africa extends south of the Langeberg–Outeniqua ranges (part of the Cape Fold Belt) from Bot River to Port Elizabeth.

The continuity of the southern Cape coast from Port Elizabeth in the east to Cape Agulhas in the west is broken by a series of logarithmic spiral bays, linked to deformation associated with Gondwana break-up (Hälbich, 1983; Watkeys, 2006). The bedrock lithology of pre-Cenozoic strata along the south coast is highly variable, creating variation in geomorphic expression (Roberts et al., 2013).

Pinnacle Point caves and rockshelters, including PP13B, are formed in the sandstone of the Skurweberg Formation (part of the Table Mountain Group) capped by various Bredasdorp marine sediments (dunes, aeolianites, calcarenites, and calcretes) (Bar-Matthews et al., 2010; Karkanas and Goldberg, 2010). PP30 is a

cave formed in the calcrete overlying the Table Mountain Group sandstone. The Paleo-Agulhas Plain now submerged off the coast includes Cretaceous Uitenhage lithologies and Mio-Pliocene limestones, cemented phosphatic rocks and ferricretes, such as the Cape St. Blaize, Cape St. Francis, and Agulhas Formations (Fig. 2) (Dingle et al., 1983; Parker and Siesser, 1972; Rogers, 1971a, 1971b).

These differences in the ages and composition of the rocks across the South Coast suggest that some should differ substantially in $^{87}Sr/^{86}Sr$ values. Previous studies that have measured $^{87}Sr/^{86}Sr$ in fauna, plants, soils, water, and rock from the GCFR (Table S1 and references therein) support this contention. For example, animals living on the Malmesbury shales in the Western Cape had $^{87}Sr/^{86}Sr$ of around 0.718 (Sealy et al., 1991), while rodents living on Bredasdorp sediments along the south coast have $^{87}Sr/^{86}Sr$ of about 0.709 (Radloff et al., 2010). This offers the possibility that strontium isotope analyses of fossil animal tissues might help resolve animal movement patterns.

2.3. Serial-sampling of teeth for isotopic analysis

Strontium isotopes have been shown to provide useful evidence for human mobility and animal movements because strontium becomes incorporated into growing tooth enamel, and does not alter after the tooth becomes fully mineralized (e.g., Ericson, 1985; Price et al., 1994; Gage et al., 1989). "Bioavailable $^{87}Sr/^{86}Sr$" that is found within the food chain derives from a combination of bedrock, soil, water, and/or atmospheric sources, and varies across landscapes. Mammalian molars grow from the apex of the tooth crown toward the neck over several months or years, incorporating the isotope ratios of the body pool into the enamel mineral lattice structure (Balasse, 2002; Passey and Cerling, 2002; Zazzo and Balasse, 2005).

There are limitations to the precision of intra-tooth isotope analysis due to attenuation of isotope values during incorporation into enamel, issues arising from sampling methods, and varying or unknown rates of tooth growth and mineralization (Balasse, 2002). Although the tooth structure is formed in a generally sequential manner from apex to neck, there are successive waves of lattice formation and mineralization that occur at different rates across the three-dimensional tooth (Balasse, 2002; Hoppe et al., 2004; Zazzo et al., 2010). Furthermore, strontium may spend time in the body pool before it becomes incorporated into the animal's tissues (Montgomery et al., 2010).

Nonetheless, intra-tooth and inter-tooth $^{87}Sr/^{86}Sr$ values have been used with success, for example, to trace the movements of modern caribou in Alaska (Britton et al., 2009), mastodons in late Pleistocene North America (Hoppe and Koch, 2007), and reindeer, bison, horse, and red deer in prehistoric Europe (Britton et al., 2011; Julien et al., 2012; Pellegrini et al., 2008; Price et al., 2015). In one prior study in the Western Cape of South Africa, strontium isotopes from archaeological sheep suggested annual movement of the animals from the coastal to inland areas (Balasse et al., 2002). If the fossil animals from Pinnacle Point were migrating across a variety of bedrock types and/or across a gradient of changing atmospheric contributions of strontium with different $^{87}Sr/^{86}Sr$ values, then intra-tooth or inter-tooth strontium isotope values should also reflect these changes.

2.4. Bioavailable strontium isotopes across the GCFR

Bioavailable strontium has not been well documented across the GCFR, but a bioavailable strontium isoscape of the region is necessary in order to test the migration hypothesis using strontium isotopes of fossil tooth enamel. Measuring $^{87}Sr/^{86}Sr$ in plants has been demonstrated to be a reliable and consistently available method for determining local bioavailable $^{87}Sr/^{86}Sr$ (Copeland et al., 2011; Durante et al., 2013; Evans et al., 2009; Maurer et al., 2012; Poszwa et al., 2009; Warham, 2011), and we employ this method to create an empirically based strontium isoscape. We have also created a geospatial model of our strontium isoscape in order to explore several issues. For example, can a geospatial model based on our empirical values be used to accurately interpolate bioavailable strontium values in areas not sampled directly by plants, such as the now-submerged Paleo-Agulhas Plain? Can it identify previously unknown factors that might control bioavailable $^{87}Sr/^{86}Sr$ or determine the best sampling strategy by which to approach future bioavailable $^{87}Sr/^{86}Sr$ studies that expand our current region?

Our approach to developing a strontium isoscape was as follows: 1) collect empirical data on modern bioavailable strontium by sampling plants across different geological substrata in the study area, 2) create a geospatial model to explore its predictive capabilities, 3) identify factors that are likely to govern the spatial structure of bioavailable $^{87}Sr/^{86}Sr$, such as geology and atmospheric sources, and 4) project this knowledge to estimate the bioavailable strontium across ancient landscapes including the exposed Paleo-Agulhas Plain.

The study area for the bioavailable $^{87}Sr/^{86}Sr$ isoscape is along the southern coast of the GCFR and aims to include the area that might have been utilized by the local and potentially migrating animals that were fossilized at the Pinnacle Point caves. The bioavailable $^{87}Sr/^{86}Sr$ sampling strategy was designed to sample multiple locations in each of the major geological groups, from the coast to the interior, and across the major physiographic units (following Marean et al., 2014). These physiographic units include the east-west trending Cape Fold Mountains, which can be divided into the southern Outeniqua Mountains and the northern Swartberg Mountains, the intermontane basin between them known as the Little Karoo, the area north of the Swartberg Mountains known as the Great Karoo (we sampled only the southern edge of this vast area), the foothills south of the Outeniqua Mountains that grade into dissected plains near the coast, and a true coastal plain, the Paleo-Agulhas Plain, that is mostly currently underwater but is preserved as isolated small remnants between the Cape Agulhas and De Hoop Nature Reserves (Thwaites and Cowling, 1988).

3. Methods

3.1. Fossil localities – PP13B and PP30

PP13B is a sea cave formed in the Table Mountain Sandstone cliffs of Pinnacle Point that has preserved MSA archaeological deposits. It has geogenic deposits that date from MIS 11 at ~400 ka to ~160 ka (Jacobs, 2010; Marean et al., 2010). Archaeological deposits in the cave date from MIS 6 (~160 ka) to 90 ka in MIS 5 when the site was sealed by a dune, and that was not breached until sometime after ~40 ka. The majority of the teeth sampled here come from sediments dated to MIS 5d and MIS 5c and during this time the coast was up to 10 km distant (Fisher et al., 2010), though there is one specimen that comes from the MIS 6 deposits, and two from the MIS 3 deposits (Table 1). People were the primary accumulators of the PP13B fauna throughout its deposition (Thompson, 2010) and hunter-gatherers exploit a daily foraging radius that is rarely greater than 10–15 km (Kelly, 1995; Marlowe, 2005).

PP30 is a paleontological site formed in the calcretes on the cliff top about 1 km from the modern coastline, and the primary accumulator was the brown hyena (*Parahyaena brunnea*). There are two optically stimulated luminescence (OSL) ages both at ~151 ka (Rector and Reed, 2010), and thus it samples a time when MIS 6 was in nearly maximum glacial conditions and the coast was far from where it is today, as much as ~95 km distant (Fisher et al., 2010). In

Table 1
List of fossil specimens analyzed from Pinnacle Point sites PP13B and PP30. Stratigraphic position (StratAggregate) and age range for PP13B are based on Marean et al. (2010), and age range for PP30 is from Rector and Reed (2010). For teeth sampled, the term "M1/M2" refers to a single tooth that could be either M1 or M2. Intra- or inter-tooth range of $^{87}Sr/^{86}Sr$ is calculated by subtracting the minimum $^{87}Sr/^{86}Sr$ value from the maximum $^{87}Sr/^{86}Sr$ value of that specimen. MIS Stage = marine isotope stage. Further details for each intra- or inter-tooth sample are available in Table S4.

Taxon	Site	Specimen #	# of intra- or inter-tooth samples	Teeth sampled	$^{87}Sr/^{86}Sr$ (mean of intra- and inter-tooth ± 1σ)	Intra-tooth range of $^{87}Sr/^{86}Sr$	MIS stage	StratAggregate	Age range (ka)
Alcelaphus buselaphus	PP13B	45264	4	M2	0.70939 ± 0.00001	0.00003	5c	DB Sand 3	91–102
		55327	4	M1/M2	0.70993 ± 0.00003	0.00007	5c	Roof Spall-Upper	91–98
		64648	4	M1/M2	0.70969 ± 0.00003	0.00007	5c	Roof Spall-Upper	91–98
	PP30	66613	3	M1/M2	0.70937 ± 0.00001	0.00002	6		151
		66615	3	M1/M2	0.70953 ± 0.00001	0.00001	6		151
		66751	3	M1/M2	0.70941 ± 0.00002	0.00004	6		151
		67209	5	M2, M3	0.70944 ± 0.00001	0.00003	6		151
		67317	3	M1/M2	0.70960 ± 0.00006	0.00012	6		151
		67502	6	M1/M2	0.70960 ± 0.00002	0.00004	6		151
Antidorcas sp. indet.	PP13B	42117	3	M1, M2, M3	0.70998 ± 0.00002	0.00004	5c	Roof Spall-Upper	91–98
		42899	4	M1, M2, M3, P4	0.70988 ± 0.00004	0.00008	5c	Roof Spall-Upper	91–98
		52675	6	M1, M2, M3	0.71002 ± 0.00001	0.00002	5c	Roof Spall-Upper	91–98
		52946	4	M3	0.70991 ± 0.00004	0.00009	5c	Roof Spall-Upper	91–98
		75112	3	M2	0.71007 ± 0.00001	0.00003	5c	Roof Spall-Upper	91–98
Antidorcas marsupialis	PP13B	22316	3	M3	0.70975 ± 0.00003	0.00006	5d	LBG Sand 1	94–134
		34638	4	M3	0.70997 ± 0.00004	0.00009	5c	DB Sand 2	91–102
		42143	3	M3	0.70945 ± 0.00001	0.00002	5c	Roof Spall-Upper	91–98
		51107	4	M1, M2	0.70979 ± 0.00003	0.00006	5c	Roof Spall-Upper	91–98
		80431	3	M1/M2	0.70990 ± 0.00002	0.00003	6	LC-MSA Lower	153–174
	PP30	66377	4	M1, M2, M3	0.70945 ± 0.00003	0.00006	6		151
		66769	4	M3	0.70943 ± 0.00001	0.00002	6		151
		66998	1	M1/M2	0.70972		6		151
		67129	3	M3	0.70942 ± 0.00001	0.00002	6		151
		115358	3	M3	0.70937 ± 0.00001	0.00001	6		151
		115387	2	M1/M2	0.70945 ± 0.00001	0.00002	6		151
Connochaetes gnou	PP13B	41399	4	M1/M2	0.71095 ± 0.00019	0.00046	5c	Roof Spall-Upper	91–98
		52943	4	M3	0.70997 ± 0.00001	0.00003	5c	Roof Spall-Upper	91–98
		53188	2	M1/M2	0.70955 ± 0.00001	0.00002	5d	LBG Sand 1	94–134
	PP30	67768	6	M1, M2, M3	0.70937 ± 0.00003	0.00006	6		151
		67867	4	M3	0.70957 ± 0.00001	0.00003	6		151
		115227	5	M3	0.70938 ± 0.00001	0.00003	6		151
		115346	2	M3	0.70957 ± 0.00002	0.00002	6		151
		115433	4	M3	0.70954 ± 0.00001	0.00001	6		151
Equus cf. *quagga*	PP30	67189	3	M3	0.70951 ± 0.00002	0.00003	6		151
Panthera leo	PP30	67374	1	P4	0.70958		6		151
Syncerus antiquus	PP13B	22929	6	M1, M2, M3	0.70963 ± 0.00006	0.00017	5c	DB Sand 2	91–102
Raphicerus campestris	PP13B	64071	1	M1/M2	0.70950		5c	Roof Spall-Upper	91–98
	PP30	66971	1	M1	0.70948		6		151
		67901	2	M3	0.70938 ± 0.00001	0.00001	6		151
		115400	3	M1, M2, M3	0.70943 ± 0.00001	0.00002	6		151
Raphicerus melanotis	PP13B	25575	1	M2	0.70930		3	Truncation Fill	35–39
		28046	1	M3	0.70927		3	Truncation Fill	35–39
		45846	2	M3	0.70934 ± 0.00003	0.00003	3	LB Silt	152–349
		79895	1	M3	0.70925		5d	Roof Spall-Lower	106–114
	PP30	66552	1	M2	0.70940		6		151
		67181	1	M2/M3	0.70946		6		151
		115223	1	M3	0.70935		6		151
Redunca arundinum	PP30	65115	2	M3	0.70937 ± 0.00001	0.00002	6		151
		67035	1	M1/M2	0.70989		6		151
		67278	3	M3	0.70939 ± 0.00002	0.00004	6		151
		67532	2	M1/M2	0.70958 ± 0	0.00000	6		151
		67535	1	M3	0.70948		6		151

Table 1 (*continued*)

Taxon	Site	Specimen #	# of intra- or inter-tooth samples	Teeth sampled	$^{87}Sr/^{86}Sr$ (mean of intra- and inter-tooth ± 1σ)	Intra-tooth range of $^{87}Sr/^{86}Sr$	MIS stage	StratAggregate	Age range (ka)
Redunca fulvorufula	PP30	66967	1	M1/M2	0.70949		6		151
		67134	2	M1/M2	0.70945 ± 0.00008	0.00011	6		151
Taurotragus oryx	PP13B	26890	3	M1/M2	0.71118 ± 0.00007	0.00013	5d	Roof Spall-Lower	106–114

contrast to the PP13B fossils that date to a variety of different time periods within the Pleistocene, all fossils from PP30 are likely to be similar in age. Brown hyenas provision their young with food, including ostrich eggs, which are abundant in the site, as well as primarily scavenged remains of large mammals. Brown hyenas are known to forage far, and in the Kalahari on average forage about 30 km at night (Mills, 1990), suggesting that their foraging radius may somewhat exceed that of people. Because of their provisioning behavior, their dens tend to accumulate bones relatively quickly.

3.2. Sampling for bioavailable $^{87}Sr/^{86}Sr$

At each of the 172 bioavailable $^{87}Sr/^{86}Sr$ sampling localities, we collected a handful of plant material from five different plants and combined those together before analysis (Table S2). In most cases, the plant growth forms present were grasses, forbs, or shrubs, so we collected a mixture of these. At four localities where there was a distinctive tree story and understory, we collected 5 plants from each and kept them as separate samples (Table S2). The plant material collected was mostly plant leaves, but also included some stems and seeds or fruits if present. All plant material was put into paper bags and allowed to dry inside the loosely packed bag.

Land snail shells were also collected at seven of the plant sampling localities. Snail shells typically contain high strontium concentrations and have been considered possible proxies for bioavailable strontium (Blum et al., 2000), but in some previous studies discrepancies were shown to exist between $^{87}Sr/^{86}Sr$ of snails versus plants (Evans et al., 2009; Maurer et al., 2012). The results of our snail samples are presented in the Supplemental Information text. We chose not to use the snail results in the development of our bioavailable strontium isoscape because of the concerns mentioned above.

Sampling localities were chosen to represent the variety of bedrock types in areas as far away as possible from disturbances such as agriculture and development. The geologist (HC), who has substantial experience in the GCFR, was present during sampling and confirmed that the local bedrock at each locality matched that identified from the 1:250,000 or 1:50,000 geological map of the region. GPS readings were taken at each sampling locality (Table S2).

3.3. Fossil specimens

We sampled a total of 55 mammalian individuals: 32 individuals from PP30 and 23 individuals from PP13B representing a total of 12 taxa (Tables 1 and 2) (Rector and Reed, 2010). The sampling strategy was designed to measure both potentially migratory and non-migratory species from the two sites, and to get serial samples for individuals through either intra-tooth sampling, sampling of successively forming teeth, or both. The dental faunal sample from PP13B is rather small, which restricted the number of individuals that we could sample. When possible, we chose to sample later forming teeth (M3) in order to ensure that the signal represents the post-weaning diet of the individual. In some cases the only available sample was M1 or M2 (or "M1/M2" when it was not possible to identify whether the tooth was M1 or M2). Several of the fossil specimens preserved multiple teeth, in which case we obtained samples from up to four teeth including the late-forming permanent premolar P4.

Information on the precise timing of tooth mineralization for the ungulates sampled in this study was not available in the published literature to our knowledge, but approximations can be made based on similar, well-studied species and reports of tooth eruption times used for age determination (Table S3). In ungulates, molars typically mineralize in a sequential manner in which enamel formation follows an uninterrupted and slightly overlapping sequence from apex to neck in permanent first molars (M1), second molars (M2), and third molars (M3). In modern cow (*Bos taurus*) and bison (*Bison bison*), M1 mineralizes over approximately 6 months from the age of 3 months before birth to 3 months old, M2 mineralizes over a year from one month old to 13 months old, and M3 mineralizes over a 15 month period from 9 to 24 months old (Brown et al., 1960; Gadbury et al., 2000). In domestic sheep (*Ovis aries*), the M1 crown forms from 2 months before birth to 6 months of age, M2 forms from 1 to 12 months of age, and M3 starts to form at 10 months and is complete by 22 months (Zazzo et al., 2010). Herbivores with very high-crowned molars have extended periods of tooth development, for example, the M1, M2, and M3 of modern domestic horses (*Equus caballus*) mineralize over periods of approximately 32 months, 30 months, and 34 months, respectively (Hoppe et al., 2004). The relatively low-crowned molars of very small steenbok (*Raphicerus campestris*) from South Africa were the subject of detailed intra-tooth carbon and oxygen isotope analysis (Balasse et al., 2002). The observed sinusoidal patterns indicate seasonal fluctuations and suggest that the steenbok M2 crown mineralized over about six months, while the M3 crown mineralized over the following six months. Published radiographs of known-age springbok (*Antidorcas marsupialis*) indicate that their molar mineralization times are very similar to that of cows and bison (Rautenbach, 1971).

Based on approximate tooth crown size and, in some cases, reported eruption patterns (see Table S3), the animals sampled in this study fall into roughly three groups in terms of permanent molar crown formation times. The first group has small molars (about 12 mm crown height) that each mineralize over about a 6 month period – these include the small steenbok (*Raphicerus campestris*) and grysbok (*Raphicerus melanotis*) (Balasse et al., 2002). The second group of species are larger and more hypsodont with crown heights for M2 and M3 around 20–30 mm. According to their eruption patterns (Table S3), these species have molar mineralization times similar to that of cows, bison, and sheep in which M1s form over about 6 months, while M2s and M3s take a year or slightly more. This second group includes hartebeest (*Alcelaphus*), springbok (*Antidorcas*), and reedbuck (*Redunca*). The third group consists of animals with very hypsodont molars with M2 and M3 crown heights on the order of 50–70 mm, similar to modern horses (Hoppe et al., 2004). In these individuals, the M1 likely takes from one to three years to form, while M2s and M3s form over about two

Table 2
Summary of the fossil animals from PP13B and PP30 sampled for strontium isotope analysis in this study.

Taxon	Common name	Feeding classification	Propensity to migrate	Number of individuals sampled from PP13B	Number of individuals sampled from PP30
Alcelaphus buselaphus	Hartebeest	Grazer	Potentially migratory	3	6
Antidorcas sp. indet.	Springbok (indeterminate species)	Browser/Mixed	Potentially migratory	5	–
Antidorcas marsupialis	Springbok	Browser/Mixed	Potentially migratory	5	6
Connochaetes gnou	Black wildebeest	Grazer	Potentially migratory	3	5
Equus cf. *quagga*	Zebra	Grazer	Potentially migratory	–	1
Syncerus antiquus	Giant buffalo (extinct)	Grazer	Potentially migratory	1	–
Raphicerus campestris	Steenbok	Browser/Mixed	Non-migratory	1	3
Raphicerus melanotis	Grysbok	Browser/Mixed	Non-migratory	4	3
Redunca arundinum	Common reedbuck	Grazer	Non-migratory	–	5
Redunca fulvorufula	Mountain reedbuck	Grazer	Non-migratory	–	2
Taurotragus oryx	Eland	Browser/Mixed	Potentially migratory	1	–
Panthera leo	Lion	Carnivore		–	1

to three years. These species include the wildebeest (*Connochaetes gnou*), eland (*Taurotragus oryx*), extinct giant buffalo (*Syncerus antiquus*), and zebra (*Equus* cf. *quagga*).

These approximations of tooth mineralization times can be used to estimate the number of seasons represented by intra-tooth or inter-tooth samples. All species analyzed in this study have sufficient intra- or inter-tooth samples to represent seasonal differences with the exception of the single *Panthera leo* sample on a P4.

3.4. Fossil sampling methods

In total, we analyzed 160 enamel and 5 dentine powder samples for strontium isotopes (Table S4). Samples of enamel powder (~4 mg) were obtained by gently abrading the side of premolars or molars using a handheld drill (UP-200 model, KUPA Inc.) equipped with a ¾ mm diameter spherical diamond drill bit (Figure S1). When possible, multiple parallel samples (up to six) were taken along the same side. The sampling line was on average 1.5–2.0 mm wide and its length was determined by the width of the tooth or lobe. The distance between the center points of intra-tooth samples was on average 5 mm, but varied from 3 to 9 mm with the exception of one *Connochaetes* specimen in which the two subsamples that produced results were 23 mm apart. For some of the smaller teeth and broken teeth, the sampling "line" was up to 5 mm wide because it was not possible to obtain enough powder from a 2 mm line, or chips of broken tooth enamel were analyzed in lieu of powder. The specifics for each case are identified in Table S4.

In the results, intra- and inter-tooth samples are presented using the "cumulative distance from neck" measurement following Price et al. (2015). The cumulative distance from neck anchors the distance from neck measurements of all the teeth from one specimen to the neck of the latest forming tooth that was sampled at zero. For each species, the maximum observed crown height (from neck to occlusal surface) for each tooth type was calculated based on the specimens in hand, and this was used to transform, for example, distance from neck measurements from M1 and M2 to cumulative distance from neck measurements that are relative to the M3. The correction factors that are based on observed crown heights are presented in Table S4. In order to visualize the approximate relative time order for the samples in Fig. 3, the results are presented on the x-axis in reverse order (M1-M2-M3-P4).

From five of the teeth on which dentine was already exposed, we took one sample of dentine powder. Comparison of $^{87}Sr/^{86}Sr$ in dentine versus enamel can be useful for assessing the possibility of diagenetic alteration of enamel strontium (Copeland et al., 2010). Unlike dentine, enamel is more resistant to diagenetic contamination because of its essentially non-porous structure with relatively large crystals and a low organic component (Budd et al., 2000; Chiaradia et al., 2003; Hoppe et al., 2003; Lee-Thorp and Sponheimer, 2003). The results of the dentine analysis are presented in the Supplemental Text and generally support the integrity of the enamel strontium in the fossil specimens from PP13B and PP30. Dentine results are also plotted alongside enamel results in Fig. 3.

3.5. Statistical analysis of the fossil isotope data

We tested for evidence of animal movements by examining strontium isotope ratios of fossil ungulate teeth in light of the bioavailable $^{87}Sr/^{86}Sr$ isoscape. For some analyses, previously identified fossil taxa (Rector and Reed, 2010) were grouped into categories based on modern observations and, in the case of extinct taxa, based on prior expectations in terms of their feeding behaviors and propensity to migrate. Animals were classified as "grazers" (primarily grass eating) or "browsers/mixed feeders," and as "potentially migratory" or "non-migratory" (Table 2). In some analyses animals were grouped according to the site from which they derived (PP13B or PP30) because the sites represent different but overlapping time periods, and had different primary collectors (humans versus hyenas). Strontium isotope values among various groupings of fossils by site, feeding behavior, taxon, and propensity to migrate are not normally distributed and some also have unequal variances. Therefore, when comparing these groups we used the non-parametric Wilcoxon test and Kruskal-Wallis test. Statistical tests were performed using JMP Pro 11.1.1 software.

3.6. Laboratory methods

Plant sample material was cut into <1 cm pieces and subsamples from each of the five plants from each sampling locality

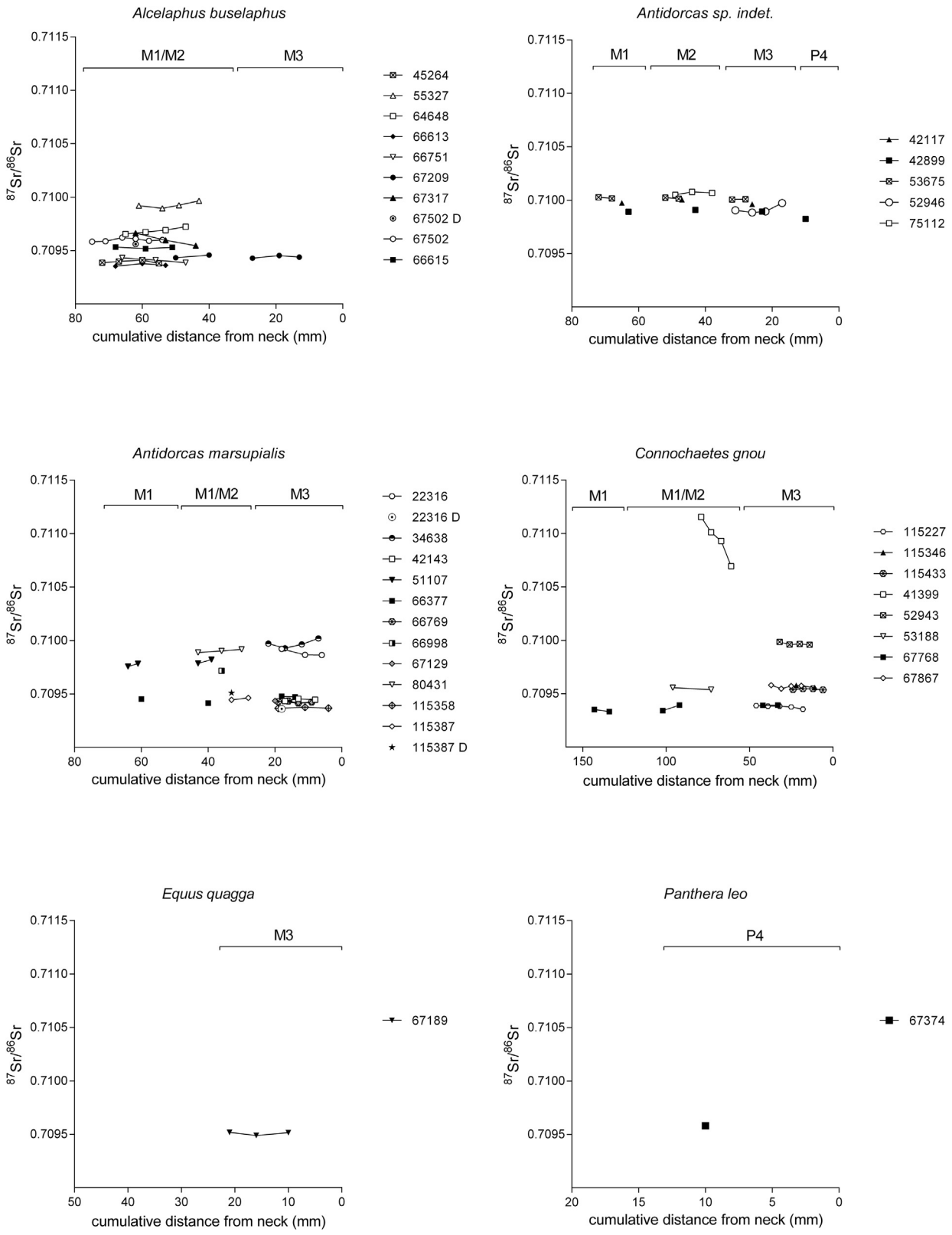


Fig. 3. $^{87}Sr/^{86}Sr$ of intra- and inter-tooth samples from fossil teeth at PP13B and PP30. The legend shows the specimen number. M1, M2, M3, P4, andM1/M2 refer to the tooth. D = dentine sample. The x-axis is cumulative distance from neck, which anchors the distance of samples from the neck of the earliest forming tooth of the specimens sampled (see text for details).

were combined in a porcelain crucible with a lid at the Department of Archaeology, University of Cape Town. Plant samples were ashed in a muffle furnace ramped at 100 °C/h to 500 °C and held at that temperature overnight.

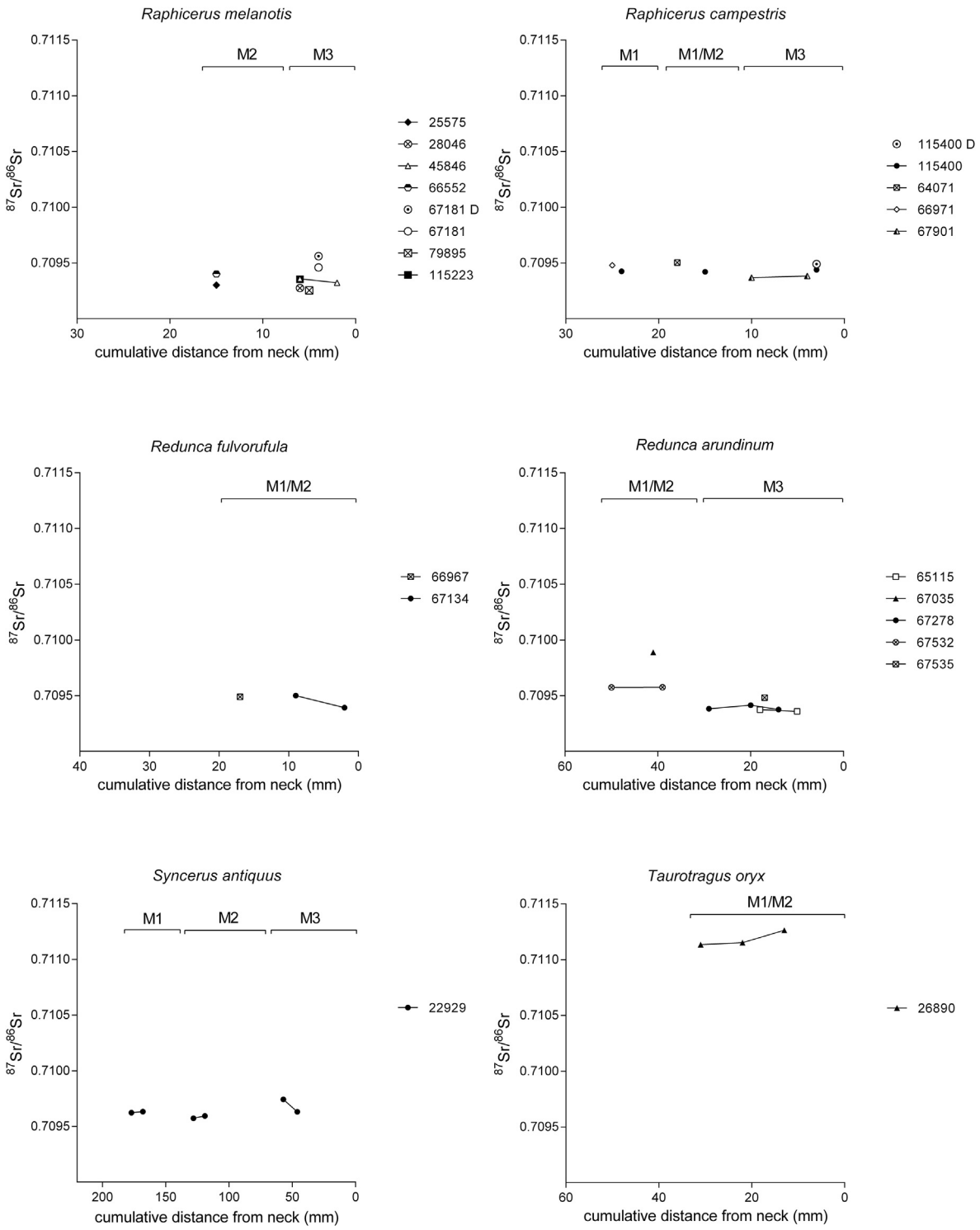


Fig. 3. (*continued*).

Strontium isotope analysis was performed in the Department of Geological Sciences at the University of Cape Town. Twenty-five mg of ashed plant material per sample was digested in 2 ml of 4:1 mixture of 48% 2B HF: 65% 2B HNO_3 in a closed Teflon beaker placed overnight on a hotplate set at 140 °C. Following two stages of dry down and re-dissolving in 1 ml 65% 2B HNO_3, 2 ml 2 M HNO_3 was added and allowed to settle overnight. 1.5 ml of liquid was pipetted out and centrifuged at 4000 rpm for 20 min, and the resulting clear supernate was collected for strontium separation chemistry. Similarly, up to 4 mg of each tooth enamel or dentine powder sample was dissolved in 2 ml 65% 2B HNO_3 in a closed Teflon beaker, and placed on a hotplate at 140 °C for an hour. It was dried down and re-dissolved in 1.5 ml 2 M HNO_3 for strontium separation chemistry. Strontium separation chemistry for all samples followed the method of Pin et al. (1994).

The separated strontium fraction for each sample was dried

down, dissolved in 2 ml 0.2% HNO_3 and diluted to 200 ppb Sr concentrations for isotope analysis using a Nu Instruments NuPlasma HR MC-ICP-MS. Analyses were referenced to bracketing analyses of NIST SRM987, using a $^{87}Sr/^{86}Sr$ reference value of 0.710255. All strontium isotope data are corrected for isobaric rubidium interference at 87 amu using the measured signal for ^{85}Rb and the natural $^{85}Rb/^{87}Rb$ ratio. Instrumental mass fractionation was corrected using the measured $^{86}Sr/^{88}Sr$ ratio and the exponential law, and a true $^{86}Sr/^{88}Sr$ value of 0.1194. Results for repeat analyses of an in-house carbonate standard processed and measured with the batches of unknown samples in this study ($^{87}Sr/^{86}Sr = 0.708920$; 2 sigma = 0.000030; n = 7) are in agreement with long-term results for this in-house standard ($^{87}Sr/^{86}Sr = 0.708907$; 2 sigma = 0.000023; n = 56).

3.7. Geospatial modeling of the strontium isoscape

We used ESRI ArcGIS 10.3 to develop a predictive model of bioavailable $^{87}Sr/^{86}Sr$ across our study area using the observed $^{87}Sr/^{86}Sr$ measurements of the modern plant samples. Fifteen percent (15%) of the original sample of data points (n = 26) were extracted from the model development and used later to test the model predictions. The remaining points (n = 148) were imported into the ESRI Geospatial Analyst to develop our variographic model predicting $^{87}Sr/^{86}Sr$ distribution across the study area. We used the ordinary kriging method because we wanted to simultaneously map the predicted values and their standard errors across the landscape. We also did not assume that the $^{87}Sr/^{86}Sr$ assumed a constant mean value across the study area. Results and further details are presented in section 4.2.

4. Results

4.1. Results of modern bioavailable $^{87}Sr/^{86}Sr$

Strontium isotope ratios of modern plants from the 172 sampling sites across the region ranged from 0.7092 to 0.7254 (Table S2). As seen in Fig. 4, bioavailable $^{87}Sr/^{86}Sr$ ratios from the Gamtoos/Malmesbury Group (0.7095–0.7157), Table Mountain Group (0.7092–0.7169), General Neogene/Quaternary deposits (0.7104–0.7162), Cape Granite Suite (0.7095–0.7177), Uitenhage Group (0.7101–0.7197), and Bokkeveld Group (0.7093–0.7209) broadly overlap. Bioavailable $^{87}Sr/^{86}Sr$ from the Cango Caves Group (0.7187–0.7254) and Witteberg Group (0.7164–0.7237) have the highest average values, and come from the northernmost portions of the study area. Bredasdorp Group samples (0.7092–0.7101) cluster tightly with the lowest average bioavailable $^{87}Sr/^{86}Sr$ and are from the coast or near the coast (up to 22 km inland) on the modern exposed Agulhas plain (Fig. 2). The Bredasdorp Group consists of marine-derived calcareous Neogene and Quaternary sediments such as beach deposits and dunes with high fractions of shell, aeolianites, and calcarenites, so its bedrock $^{87}Sr/^{86}Sr$ is expected to be close to the Quaternary marine value of 0.7092. Overall, the range of strontium isotope ratios within calcareous rocks tends to be less than in non-calcareous rocks.

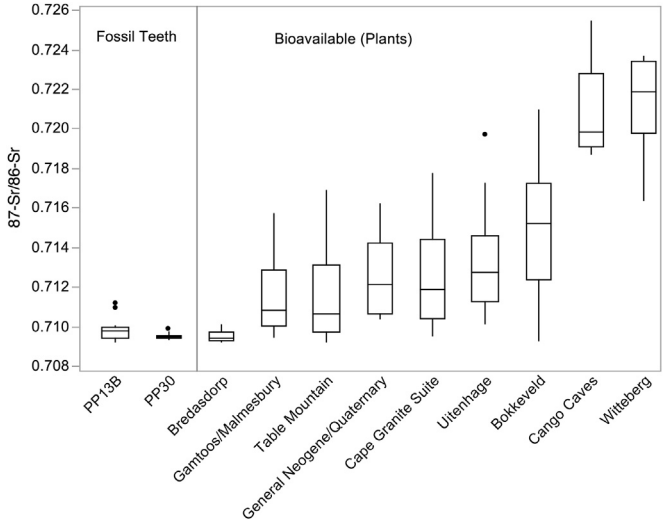


Fig. 4. $^{87}Sr/^{86}Sr$ of fossil tooth enamel from PP13B and PP30 and bioavailable $^{87}Sr/^{86}Sr$ as measured by plants across the modern landscape. Plants are grouped according to the geological group of the bedrock at the sampling locality. Boxes show the median value and 25th and 75th quartiles, whiskers extend by 1.5 times the interquartile range, and all outliers are shown.

Although bioavailable strontium isotope ratios vary within most of the geological groups, there is an overall pattern of increasing $^{87}Sr/^{86}Sr$ with increasing distance from the coast. Distance to coast is a stronger predictor of bioavailable $^{87}Sr/^{86}Sr$ ($R^2 = 0.77$) than latitude alone ($R^2 = 0.68$), while longitude shows almost no relationship ($R^2 = 0.03$) (Fig. 5). Bioavailable $^{87}Sr/^{86}Sr$ from localities directly on the coast have the lowest values approaching that of modern seawater (0.7092) regardless of geology. For example, plants sampled from the modern exposures of the Agulhas Plain have $^{87}Sr/^{86}Sr$ ratios of 0.7092–0.7107 and are mainly from Bredasdorp Group sediments, but some were growing on Bokkeveld Group, Table Mountain Group, and Uitenhage Group geological substrates (Fig. 2). Sampling localities on the dissected coastal plain have intermediate plant values of 0.7095–0.7172, and occur on Table Mountain Group, Bokkeveld Group, Uitenhage Group, Cape Granite Suite, and Gamtoos/Malmesbury Group geological substrates. Sampling sites from the intermontane basin (Little Karoo) have plant $^{87}Sr/^{86}Sr$ ranging from 0.7124 to 0.7202, and occur on Table Mountain Group, Bokkeveld Group, Uitenhage Group, General Neogene/Quaternary deposits, Cango Caves Group, and Witteberg Group geological substrates. Sampling sites from northernmost portions of our study area, north of the Swartberg Mountains in the Great Karoo, have plant $^{87}Sr/^{86}Sr$ ranging from 0.7168 to 0.7237, and occur on Table Mountain Group, Bokkeveld Group, and Witteberg Group geological substrates. Samples within the Cango Caves Group and the Witteberg group, which are at least 65 and 78 km away from the coast, respectively, show a weak or inverse relationship of $^{87}Sr/^{86}Sr$ with distance to coast (Figure S2).

4.2. Results for geospatial modeling of the strontium isoscape

The geospatial distribution of bioavailable $^{87}Sr/^{86}Sr$ is skewed heavily towards values <0.7110. Samples having values <0.7110 were located entirely within 20 km of the current coastline and likely indicate a zone of increased marine influence on bioavailable $^{87}Sr/^{86}Sr$. Otherwise, intragroup analysis of the localities grouped by <20 km and >20 km from the modern coastline showed more normally distributed $^{87}Sr/^{86}Sr$ values.

We fitted different semivariogram models to the data and observed the prediction errors. Testing for various semivariograms and their parameters revealed that the $^{87}Sr/^{86}Sr$ values were anisotropic on a bearing of ~78°, which is roughly in line with the orientation of the Cape Fold mountains, the generally east-west trending geological strata, and the modern coastline. A spherical semivariogram provided the smallest mean (−0.0000) and standardized mean (−0.0015), indicating unbiased prediction errors. The root mean squared prediction errors were also low (0.0017) and only differed from the average standard error (0.0013) by a value of 0.0004, which indicates a robust assessment of variability

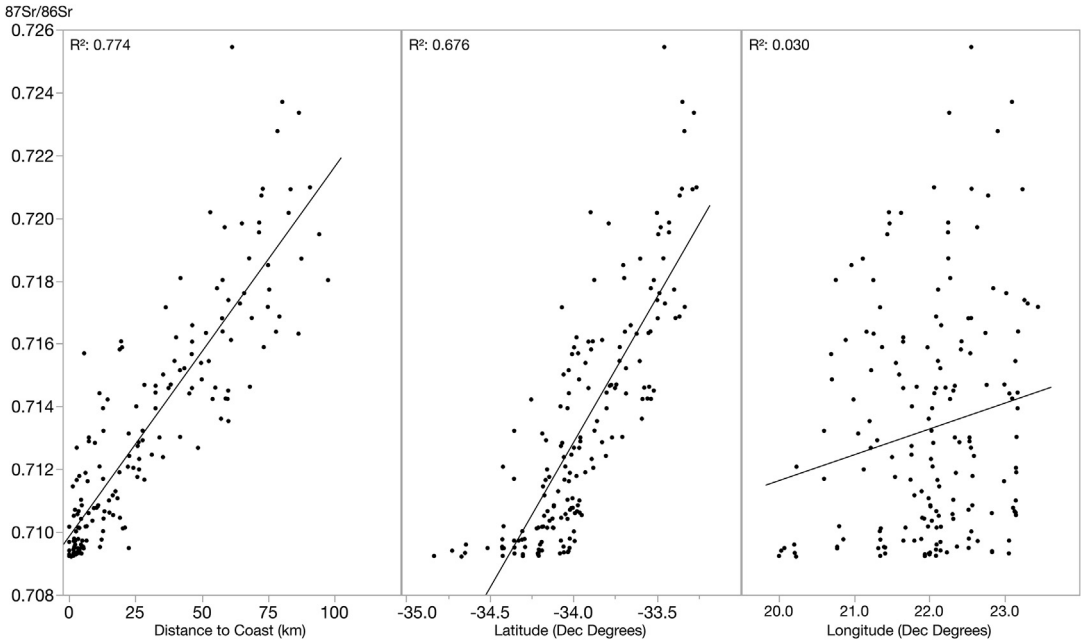


Fig. 5. Bioavailable $^{87}Sr/^{86}Sr$ from the modern sampling localities plotted relative to distance to the modern coastline, latitude, and longitude.

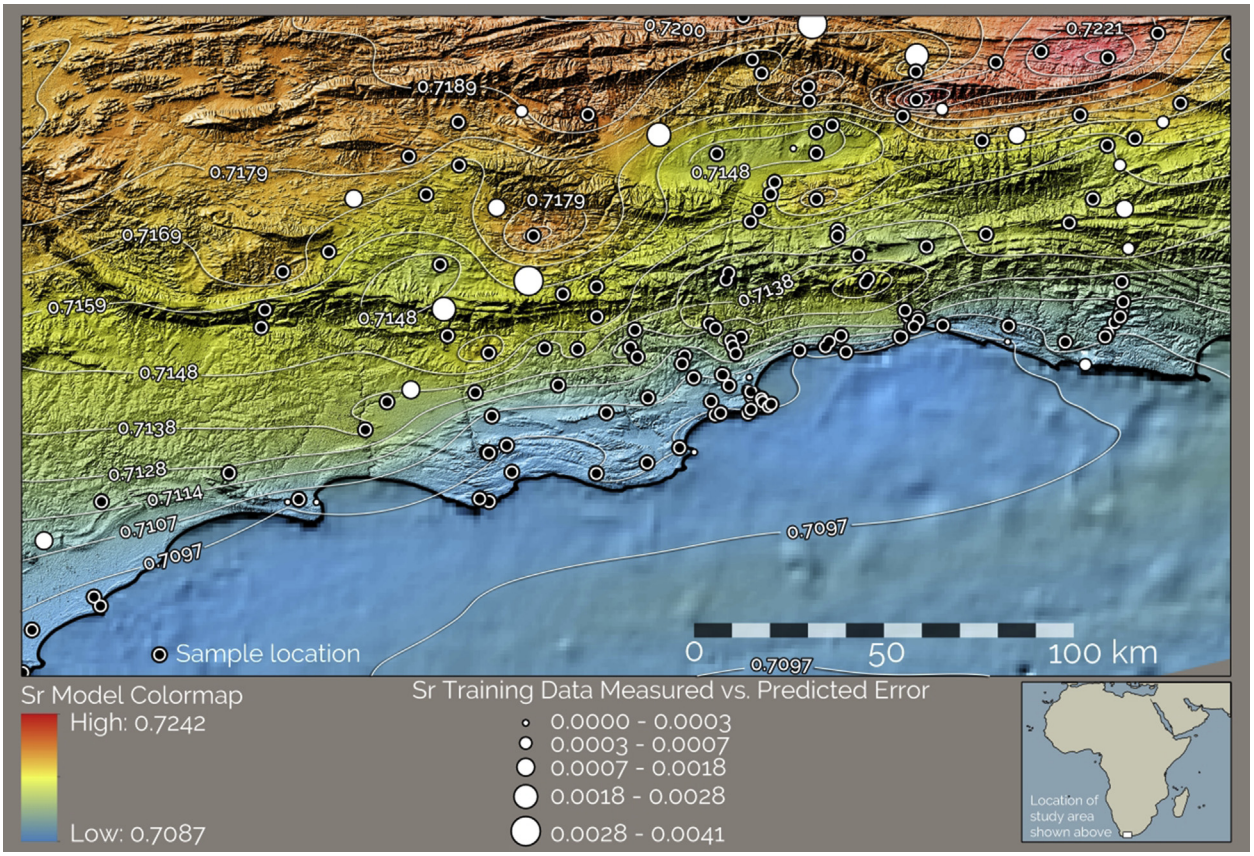


Fig. 6. Bioavailable strontium isoscape ($^{87}Sr/^{86}Sr$) predictive geospatial model developed in ESRI ArcGIS 10.3. Circles with black dots in the center represent bioavailable $^{87}Sr/^{86}Sr$ sampling localities used to create the model. White dots represent the 26 randomly selected sampling locations that were extracted prior to model development and used later to test the model predictions. The size of the white dots shows the amount by which measured $^{87}Sr/^{86}Sr$ differed from the model's predictions. Contour lines show the predicted bioavailable $^{87}Sr/^{86}Sr$ based on the model. Colors indicate areas of lowest bioavailable $^{87}Sr/^{86}Sr$ (blue) to highest bioavailable $^{87}Sr/^{86}Sr$ (red). (For interpretation of the references to color in this figure legend, the reader is referred to the web version of this article.)

in the model predictions. The model parameters and results are provided in Table S5 and S6. The final bioavailable $^{87}Sr/^{86}Sr$ geospatial model is shown in Fig. 6.

When the variability in the standard error from the model predictions is mapped across the study area it is fairly evenly distributed. That variability is likely to be underestimated subtly, however, as indicated by the slightly elevated standardized root mean square value of 1.3102. Moreover, we observed that there was a rapid increase in the standard error of the model predictions approximately 25 km away from the sample locations. In normally distributed datasets, accurate predictions should occur within 2× the average standard error 95% of the time. The ~25 km buffer coincided with the 0.0026 isohyet, which is 2× our average standard error, and thus it can be used to demarcate reliable (<0.0026) and unreliable (>0.0026) model predictions. We used this 25 km buffer to exclude model predictions that we consider to be unreliable.

After the model was created it was validated using the subset of points removed from the original dataset. The absolute difference between the subset $^{87}Sr/^{86}Sr$ values and model predictions is small – having a mean of 0.0012 – and also consistent with a standard deviation of just 0.0012.

Thereafter, we projected 100,000 points randomly across the study area and extrapolated the predicted model results at each of these locations. We also derived the lithological group at each point by spatially joining these points to the 1:250,000 geological classifications provided by the South African Council for Geoscience. All points from areas that fell outside of our 25 km buffer were subsequently removed, which resulted in a total data set of 68,338 points for comparisons.

We grouped these 68,338 points by geology and compared the mean predicted values with the mean observed values (empirically measured plants) from each geological type. These data are included in Table S5 alongside the predicted descriptive statistics from the geospatial model. The absolute differences between the observed and predicted mean $^{87}Sr/^{86}Sr$ values for each geological group ranged up to 0.0053 (Gamtoos/Malmesbury Group), but in general were low ($\bar{x} = 0.0022$, $sD = 0.0018$, $p = 0.001$). Linear regression between the observed and predicted bioavailable $^{87}Sr/^{86}Sr$ values resulted in $R^2 = 0.52$ ($p < 0.05$). When the Gamtoos/Malmesbury Group and Cango Cave Group points (related geologically) were removed from the regression then the $R^2 = 0.73$ ($p < 0.05$).

4.3. Results for $^{87}Sr/^{86}Sr$ of fossil teeth

The strontium isotope ratios of tooth enamel from the 55 fossil individuals from PP13B and PP30 fell within a range that is considerably smaller than that of the modern plants (Fig. 4). Fifty-three individuals had $^{87}Sr/^{86}Sr$ from 0.7092 to ~0.7101, while one wildebeest and one eland had higher ratios of ~0.7110. In general, the strontium isotope ratios were far more variable between individuals than within serial samples from each individual (Fig. 3). Among all individuals with two or more intra- or inter-tooth samples, the average difference between maximum and minimum serial $^{87}Sr/^{86}Sr$ ratios was 0.00006.

Strontium isotope ratios of animals from PP13B considered as a group (0.7098 ± 0.0005, n = 23) were significantly higher than those from PP30 (0.7094 ± 0.0001, n = 32; p = 0.003). Potentially migratory animals (Table 1) at PP13B (0.7099 ± 0.0005) had on average higher $^{87}Sr/^{86}Sr$ than non-migratory animals from the same site (0.7093 ± 0.0001, p = 0.002), but this pattern was not found at PP30 (potentially migratory animals 0.7095 ± 0.0001; non-migratory animals 0.7095 ± 0.0001). There was no difference in $^{87}Sr/^{86}Sr$ between species typically considered grazers versus those typically considered browsers and/or mixed feeders at either PP13B (grazers 0.7099 ± 0.0004; browsers 0.7097 ± 0.0006; p = 0.06) or PP30 (grazers 0.7095 ± 0.0001; browsers 0.7094 ± 0.0001; p = 0.16).

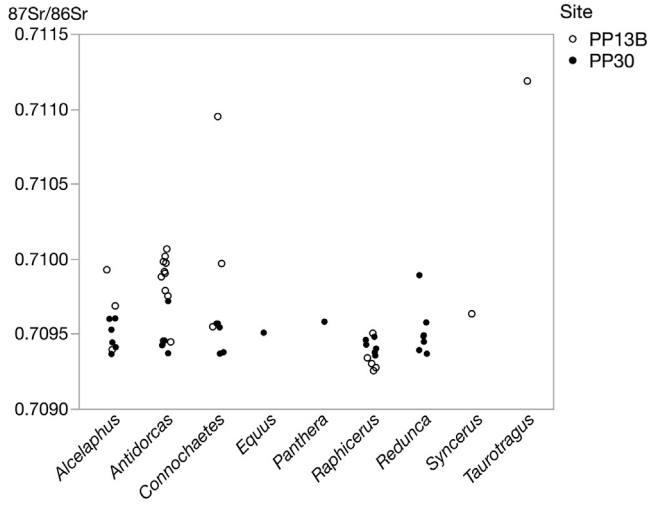


Fig. 7. Results of fossil enamel samples by genus and site. Each point represents the average of all intra- and inter-tooth samples from one specimen as reported in Table 1.

There are differences between $^{87}Sr/^{86}Sr$ by genera when specimens from both sites are combined (Kruskal-Wallis Test; genera with only one individual excluded; p = 0.0046) (Fig. 7). A Wilcoxin test on each pair (one-tailed) indicates that *Raphicerus* has lower $^{87}Sr/^{86}Sr$ than *Alcelaphus* (p = 0.008), *Antidorcas* (p = 0.001), *Connochaetes* (p = 0.004), and *Redunca* (p = 0.023). Among genera represented by more than one individual, *Connochaetes* and *Antidorcas* have the highest variances between individuals and *Raphicerus* has the lowest variance between individuals.

4.3.1. Results by taxon

We sampled nine *Alcelaphus buselaphus* (hartebeest) individuals, six from PP30 and three from PP13B (Figs. 3 and 7). The hartebeest is a plains antelope that is often migratory, though less so than wildebeest (Estes, 1991). The $^{87}Sr/^{86}Sr$ values are moderately variable between individuals, but inter- and intra-tooth variation is always less than 0.0001 in samples that represent 3–12 months of tooth formation.

We sampled eleven individuals of the extant springbok species (*Antidorcas marsupialis*), five from PP13B and six from PP30, and five springbok of undetermined species (*Antidorcas* sp. indet.), all from PP13B. The extant springbok is a plains antelope that is typical of treeless landscapes, ranges across a wide variety of habitats, and has been known to migrate in vast herds (Skead, 2011). The sampled specimens have a relatively broad range of values, and those from PP13B are higher than those from PP30 (p = 0.002) (Fig. 7). Inter- and intra-tooth variation that represents more than six months of time (15 mm across the M3) on at least five individuals does not exceed 0.00009.

We sampled eight *Connochates gnou* (black wildebeest), three from PP13B and five from PP30. The black wildebeest is a true plains antelope and is typically migratory (Estes, 1991). Specimen 41399 from PP13B has the greatest amount of intra-tooth variation (0.00046) seen within any single individual of the project, and has anomalously high values (mean = 0.71116). Its intra-tooth samples span 18 mm of the M1/M2 (one half to one third of the total crown height), which represents about 3–9 months of mineralization time (Table S3). For four other wildebeest specimens, intra-tooth

samples spanning >18 mm on the M3 represent approximately 6–12 months of mineralization time, but the maximum intra-tooth variation for these is only 0.00003. Wildebeest have the highest variance between individuals of all genera.

Raphicerus (steenbok and grysbok) are small, sedentary antelopes with restricted local home ranges (Skinner and Smithers, 1990). The 11 individuals that we sampled have consistently low $^{87}Sr/^{86}Sr$ values (0.70925–0.70950) below the mean $^{87}Sr/^{86}Sr$ for individuals of all taxa (0.70962; n = 55). Steenbok and grysbok have the lowest variance between individuals of all genera (Fig. 7).

We sampled five *Redunca arundinum* (southern reedbuck) and two *Redunca fulvorufula* (mountain reedbuck), all from PP30. Both are grazers, the former specializing on wet edaphic grasslands and the latter on grassy slopes (Estes, 1991). Although reedbuck are also non-migratory, their mean $^{87}Sr/^{86}Sr$ values are higher ($p = 0.023$) than those of *Raphicerus*.

We sampled the only available molar from *Equus* cf. *quagga* (zebra), which was an M3. Three intra-tooth samples spanning 11 mm, or about 3–6 months of mineralization time, show a $^{87}Sr/^{86}Sr$ value of 0.70951 with an intra-tooth range of 0.00003. The zebra is a plains animal that is sometimes migratory.

We sampled one extinct giant buffalo (*Syncerus antiquus*) mandible. The extinct giant buffalo is thought to have been a plains grazer due to its hyper-hypsodont tooth row (Klein, 1994). We took two intra-tooth specimens each from the M1, M2, and M3, which show relatively low variation (0.00017) and a mean $^{87}Sr/^{86}Sr$ value of 0.70963. The time "missing" between the samples on each tooth could be up to a year or more.

We sampled a single *Taurotragus oryx* (eland) M1/M2 with three intra-tooth samples that represent about 3–6 months of mineralization time. Intra-tooth variation is 0.00013 and the $^{87}Sr/^{86}Sr$ value is extremely high, matched only by one wildebeest specimen.

We sampled a single *Panthera leo* (lion) from PP30 on its P4. Its $^{87}Sr/^{86}Sr$ value (0.70958) is extremely close to the mean $^{87}Sr/^{86}Sr$ for individuals of all taxa (0.70962; n = 55).

5. Discussion

5.1. Bioavailable strontium isoscape

The range of bioavailable strontium isotope ratios documented in plants across the south coast portion of the modern GCFR is 0.7092–0.7254 (Figs. 4 and 6). This is consistent with expectations, given that the end members of this system are strontium contributed from modern seawater (0.7092), and bedrock-derived strontium from either soil or dust. The bedrock-derived strontium from Bredasdorp limestone and other marine sediments along the modern coastline, and across much of the now-submerged Paleo-Agulhas Plain, should have $^{87}Sr/^{86}Sr$ ratios around 0.7092, since they derive predominantly from marine organisms. However, strontium from the Precambrian and Paleozoic bedrock that forms most of the Cape Fold Mountains and surrounding areas should have much higher $^{87}Sr/^{86}Sr$ ratios (Table S1). Published measurements of Malmesbury shale whole rock $^{87}Sr/^{86}Sr$ range from 0.721 to 0.787, consistent with expectations for a rock that is ancient and has relatively high rubidium to strontium ratios (Allsopp and Kolbe, 1965; Backeberg et al., 2011). Similarly, Cape Granite Suite whole rock $^{87}Sr/^{86}Sr$ ranged from 0.77 to 1.16 (Allsopp and Kolbe, 1965), and bedrock $^{87}Sr/^{86}Sr$ from the Table Mountain Group measured 0.747 (Midgley et al., 2012). Although the strontium that becomes part of the bioavailable nutrients in soil as a result of bedrock decomposition may not have the same $^{87}Sr/^{86}Sr$ ratio as the parent whole rock values (Sillen et al., 1998), bedrock or dust-derived strontium from the Cape Fold Mountains and surrounding areas should nevertheless be substantially higher than modern marine values of 0.7092.

The strong correlation between bioavailable $^{87}Sr/^{86}Sr$ and distance to coast implies a heavy influence of marine-derived strontium (0.7092) to the bioavailable pool on the south coast portion of the modern GCFR (Fig. 5, Figure S2). Marine-derived strontium has been shown to contribute substantially to bioavailable strontium in coastal regions around the world (Chadwick et al., 2009; Evans et al., 2010; Whipkey et al., 2000). Marine-derived strontium can be added to the onshore biosphere either directly as sea spray at or very near the coast, or more indirectly further inland in the form of fog and precipitation that derives from marine sources (Montgomery, 2010). Seawater (~8–9 ppm Sr) and sea salt (~22 ppm Sr) have considerably higher concentrations of strontium than most freshwaters (many are < 1 ppm Sr; Chesson et al., 2012; Culkin and Cox, 1966; Fenner and Wright, 2014; Horne, 1969; Montgomery et al., 2006; Odum, 1957; Voerkelius et al., 2010).

Most large intercontinental dust plumes are in the equatorial region or northern hemisphere, where they contribute strontium to biospheres in Hawaii, the Caribbean, and the eastern Mediterranean, among other places (Bataille et al., 2012; Chadwick et al., 2009; Hartman and Richards, 2014). There is less dust in the southern hemisphere overall (Bryant et al., 2007; Vickery et al., 2013). While dust may contribute some strontium to the GCFR system (Soderberg and Compton, 2007), much of that dust is likely to be derived from local bedrock sources, thereby also containing local bedrock-derived $^{87}Sr/^{86}Sr$. Some dust may also come from the semi-arid Great Karoo north of the GCFR, which also has relatively high $^{87}Sr/^{86}Sr$ (de Villiers et al., 2000; Midgley et al., 2012).

Bioavailable $^{87}Sr/^{86}Sr$ along the south coast of the GCFR could change over time if the relative contribution of strontium from marine versus bedrock or dust changed. Since distance to coast from the Pinnacle Point caves has varied from 0 to 100 km throughout the late Pleistocene (Fisher et al., 2010), this is a possibility worthy of consideration. We can estimate the magnitude of change in bioavailable $^{87}Sr/^{86}Sr$ with changes in distance to coast using the $^{87}Sr/^{86}Sr$ measured in time sequence in speleothems from caves at Pinnacle Point as reported in Fisher et al. (2010). Speleothems are formed from seepage water within the caves, and the strontium within that seepage water likely derives from a combination of sources such as soil, bedrock, dust, sea spray, fog, and precipitation. As such, the $^{87}Sr/^{86}Sr$ ratios in speleothems are likely a good reflection of bioavailable $^{87}Sr/^{86}Sr$.

Fisher et al. (2010) found that $^{87}Sr/^{86}Sr$ in speleothems from Pinnacle Point caves dating from ~325 ka to the present vary through time as a function of distance from coast, as predicted by a model in which atmospheric marine-derived strontium contributes substantially to speleothem (and bioavailable) $^{87}Sr/^{86}Sr$. When the coast is very near, $^{87}Sr/^{86}Sr$ ratios in the speleothems tend to approach ~0.7092, the value of modern seawater, while greater distances to the coast (up to 100 km) correspond to higher values with a maximum of 0.70965 (Fisher et al., 2010), due presumably to a greater relative contribution of bedrock- or dust-derived strontium. However, this magnitude of change (~0.0005) is small relative to the variability of bioavailable strontium isotope ratios across the entire region (0.7092–0.7254). It is less than the difference between some modern plants growing on the Bredasdorp Group calcareous sediments (0.7092–0.7011). It is comparable to the maximum intra-tooth variability observed in one fossil wildebeest from PP13B (0.00046). Thus, the low magnitude of change in speleothem $^{87}Sr/^{86}Sr$ over the past 325 ka despite movement of the coast by 100 km indicates that modern bioavailable $^{87}Sr/^{86}Sr$ in the area around and north of the current coastline is a robust representation of bioavailable strontium distribution in the past. Although sea level changes may have resulted in shifts in bioavailable $^{87}Sr/^{86}Sr$ at the coast of ~0.0005 at and near the coast,

this shift is insignificant compared to differences between bioavailable $^{87}Sr/^{86}Sr$ near the coast versus near the Outeniqua Mountains, for example.

In order to reconstruct bioavailable strontium isotope values across the now-submerged Paleo-Agulhas Plain, we draw upon evidence of the offshore geology, what we have learned about how marine- and bedrock-derived strontium interact on the current land surface, and predictions of the geospatial model.

5.2. Paleo-Agulhas plain bioavailable strontium isoscape

Although the present-day submerged Agulhas Bank is a highly eroded (Martin and Flemming, 1986), oceanic current-dominated continental shelf (Johnson and Baldwin, 1986), preserved Quaternary deposits include aeolianite, beach deposits, infilled river channels and buried back-barrier sediments (Cawthra et al., 2014). Using seismic and surficial geological data, Cawthra (2014; Cawthra et al., 2015) showed that during the sea-level lowstand of MIS 6, shallowly incised rivers with broad adjacent floodplains dominated the Paleo-Agulhas Plain, particularly in the vicinity of Mossel Bay (5 km east of Pinnacle Point). A high abundance of carbonate in the system suggests active dune sedimentation at this time, with likely exposure of the Neogene limestone deposits. The successive glacial periods of MIS 4 and MIS 2 are interpreted to be associated with a larger sediment supply of unconsolidated Bredasdorp Group sediments. Broad paleo-coastal zones of dunefields likely swept the shelf at these times, burying the older geological lithologies (Cawthra, 2014).

The hard-rock geological composition of the shelf beneath the modern marine sediment wedge is characterized by a coast-parallel trending outcrop of Uitenhage Group (Cretaceous) deposits directly adjacent to the modern coastline, immediately south and east of Pinnacle Point with an additional component along the modern coast further to the west (Fig. 2). Modern on-shore Uitenhage Group exposures along the South Coast have bioavailable $^{87}Sr/^{86}Sr$ from 0.7101 to 0.7197. The three Uitenhage sites that are less than 4 km from the modern coast, and presumably have the greatest influence of marine-derived strontium, have the lowest bioavailable $^{87}Sr/^{86}Sr$ ratios of 0.7101. The modern Uitenhage range may be our best estimation of the bioavailable $^{87}Sr/^{86}Sr$ range of Uitenhage exposures on the Paleo-Agulhas Plain when this bedrock was exposed at the surface. At times, marine sands in the form of dunes, aeolianites, and other calcareous sediments may have buried the offshore Uitenhage Group bedrock (Cawthra, 2014) and contributed strontium to the biosphere with $^{87}Sr/^{86}Sr$ close to 0.7092. However, when Quaternary sediments were stripped off the Cretaceous shales, the soils derived from these rocks would have been fertile and would have likely supported Renosterveld with a varying but generally high component of C4 grasses (Cowling, 1983; Cowling and Potts, 2015), depending on the amount of warm season rainfall. The modern, near-shore Uitenhage sampling localities provide an estimate for bioavailable $^{87}Sr/^{86}Sr$ (0.7101) for exposed Cretaceous shales.

South of the offshore Uitenhage Group deposits are belts of the Cape St. Blaize- and Cape St. Francis Group sediments, that do not have equivalent exposures on the contemporary coast (Fig. 2). Both are predominantly Palaeogene and Neogene limestones and calcareous clays (Dingle et al., 1983) and therefore are likely to have whole rock $^{87}Sr/^{86}Sr$ ratios of approximately 0.7092 or slightly higher, with bioavailable $^{87}Sr/^{86}Sr$ similar to the Bredasdorp Group (0.7092–0.7101). The Cape St. Blaize- and Cape St. Francis Groups offshore were also likely covered in dune sands that would further contribute toward a bioavailable $^{87}Sr/^{86}Sr$ ratio close to 0.7092.

Approximately 100 km southwest of Pinnacle Point on the Paleo-Agulhas Plain, bedrock zones that may have been exposed at lower sea levels include Uitenhage Group deposits, the Alphard Igneous Complex, Bokkeveld Group shales, and Table Mountain Group sandstones (Fig. 2). Based on direct analogy with their modern onshore counterparts, the Uitenhage-, Bokkeveld-, and Table Mountain Group areas could have had bioavailable $^{87}Sr/^{86}Sr$ ratios ranging from 0.7092 to 0.7209. However, it is likely that they were covered either totally or partially in marine sands and influenced by direct sea spray or marine-derived precipitation, all of which would tend to bring bioavailable $^{87}Sr/^{86}Sr$ lower, closer to 0.7092. The Alphard Igneous Complex is composed of Tertiary volcanic tuff, trachyte, and basalt (Dingle et al., 1983). As expected for young volcanics, its whole rock strontium ratios are extremely low, around 0.7029 (Janney et al., 2002).

In sum, it is likely that most of the Paleo-Agulhas plain had bioavailable $^{87}Sr/^{86}Sr$ similar to, or even at the low end of, the modern Bredasdorp Group range of 0.7092–0.7101. The Palaeogene and Neogene-aged Cape St. Blaize- and Cape St. Francis Groups were likely to have whole rock values close to 0.7092. The Precambrian and Paleozoic bedrock geologies on the Paleo-Agulhas plain (e.g., Bokkeveld and Table Mountain Groups) likely have whole rock $^{87}Sr/^{86}Sr$ ratios that are much higher. However, seismic and surficial geophysical evidence on the South Coast (Cawthra et al., 2014, 2015) suggests that on the inner- and mid-shelf they were mostly covered with marine sands, aeolianites, or other calcareous sediments during times of lowered sea level. This sediment cover, along with marine-derived sea-spray, fog, and precipitation, likely swamped the bioavailable strontium isotope ratio, as is the case in current outcrops of these rocks near the coast. It is unlikely that anywhere on the Paleo-Agulhas Plain bioavailable $^{87}Sr/^{86}Sr$ ratios were higher than the range of the fossil animals with the possible exception of the older bedrock areas >100 km southwest of Pinnacle Point.

5.3. Implications for fossil animal movements

Comparison of $^{87}Sr/^{86}Sr$ values of the fossil animals analyzed from PP30 and PP13B to the isoscape model suggests that the animals spent little or no time substantially north of the current coastline. The predominant range of strontium isotope values in the fossils (0.7092–0.7101) is consistent with bioavailable strontium isotope ratios on modern exposures of Bredasdorp Group and the coastal plain, including some sites on Table Mountain Group, Bokkeveld Group, Cape Granite Suite, and Gamtoos/Malmesbury Groups near the coast (see similar results in Radloff et al., 2010). The fossil values are also consistent with most areas of the Paleo-Agulhas Plain when it was exposed, as suggested by our strontium isoscape model. Since there is no reason to infer that bioavailable $^{87}Sr/^{86}Sr$ of the interior (the dissected plain, Cape Fold Mountains, Little Karoo, and Great Karoo) ever received a greater contribution of marine-derived strontium than at present, interior bioavailable strontium isotope ratios have probably been the same as today or higher since MIS 6. The two animal individuals from PP13B with the highest $^{87}Sr/^{86}Sr$ ratios of ~0.711 (a wildebeest and an eland) could have spent time on the dissected plain, but probably spent very little or no time in the area north of the Outeniqua Mountains, which has bioavailable $^{87}Sr/^{86}Sr$ ranging from 0.712 to 0.724, at least while their teeth were mineralizing. Taken together, the pattern suggests that grazing opportunities on the Paleo-Agulhas Plain were considerably more attractive than areas to the north of the modern coastline.

The low intra-tooth strontium isotope variability in nearly all individuals (Fig. 3) suggests either that they were not moving much during the time of tooth formation, or that if they were moving, it was along a region of relatively constant bioavailable strontium isotope ratios. Since bioavailable $^{87}Sr/^{86}Sr$ varies with a strong

gradient from south to north (at least north of the modern coastline), but not from east to west, the unchanging intra-tooth values of nearly all fossil individuals could be consistent with east-west movements. However, they are inconsistent with large north-south movements in the region north of the modern coastline. Several of the species analyzed are known to migrate long distances (wildebeest, springbok, zebra), so unless their behaviors were substantially different in the Pleistocene, east-west movements are still a strong possibility. Additional analyses using carbon isotopes might help to resolve this issue since the proportion of C_4 grasses increases from west to east (Cowling, 1983; Vogel et al., 1978).

Animals from PP13B (0.7098 ± 0.0005) have higher $^{87}Sr/^{86}Sr$ ratios than animals from PP30 (0.7094 ± 0.0001). This could be due to differences in the areas of the landscape used by animals and/or differences in bone accumulators at these two sites. PP30 dates to 151 ka when sea level was lower and the coast is modeled to be 95 km away (Fisher et al., 2010). PP13B fauna come from several different time periods, but the biggest sub-sample (n = 11) is from the "Roof Spall-Upper" stratigraphic aggregate that dates to 91–98 ka when the coast is modeled to be less than10 km away (Fisher et al., 2010). Within the Roof Spall-Upper stratigraphic aggregate, shellfish assemblages collected by people include substantial portions of both sandy beach and rocky intertidal zone species, suggesting that the coast was within the daily foraging radius of hunter-gatherers, which rarely exceeds 10–15 km. If local bioavailable $^{87}Sr/^{86}Sr$ at Pinnacle Point itself changed slightly with sea levels along the magnitude suggested by changes in the PP speleothems (~0.0005) (Fisher et al., 2010), then we would expect slightly higher values during PP30 times when the coast was further away.

Since the PP30 animals actually have lower $^{87}Sr/^{86}Sr$ than the PP13B animals, the PP30 animals were probably spending most of their time on the widely exposed Paleo-Agulhas Plain with its relatively low strontium isotope ratios. In contrast, some PP13B animals may have been forced to spend more time in the immediate vicinity and north of the modern coastline because a smaller extent of the Paleo-Agulhas Plain would have been exposed during their lifetimes. This would mean that the animals sampled at PP13B foraged further onto the dissected plain where there are a greater variety of rock types, fewer calcareous rocks, and higher bioavailable strontium isotope ratios. The fact that the wildebeest and eland with the highest $^{87}Sr/^{86}Sr$ values are both from PP13B is consistent with this interpretation.

During the accumulation of PP30, the coastal plain was so large that it may have supported a large mammal ecosystem. In the modern and historic GCFR, Renosterveld is regarded as the biome best able to support a large biomass of grazers (Boshoff et al., 2001; Boshoff and Kerley, 2001). Renosterveld occurs across the dissected plain north of the modern coastline on the relatively high $^{87}Sr/^{86}Sr$ Bokkeveld shales. It may have been present on portions of the exposed Paleo-Agulhas Plain near the modern coastline if Quaternary sediments were stripped from the Cretaceous shales, contributing to localized areas of slightly higher bioavailable $^{87}Sr/^{86}Sr$. That animals during PP30 times appear to have been using the Paleo-Agulhas Plain and not the dissected plain, even though the site of PP30 itself is along the border of these two landforms, suggests that the Paleo-Agulhas plain provided the preferred habitats.

Another possible explanation for the slightly higher $^{87}Sr/^{86}Sr$ at PP13B could be related to the differing accumulators, which were humans at PP13B and brown hyenas at PP30. It is possible that humans were hunting further afield and in a wider variety of habitats such as those found in the dissected plain, while the hyenas at PP30 focused only on the Paleo-Agulhas Plain. Even if this were the case, however, the overall trend of low $^{87}Sr/^{86}Sr$ values among the animals relative to bioavailable $^{87}Sr/^{86}Sr$ across the broader region implies that in general they preferred Paleo-Agulhas Plain or modern coastline areas over areas further to the north.

Among comparisons between the various animal genera, the only statistically significant difference is that small *Raphicerus* antelopes have lower strontium isotope values that are tightly clustered, regardless of whether they are from PP30 or PP13B. Since *Raphicerus* are known to have small home ranges and are territorial, these animals may be more representative of the "local" bioavailable strontium isotope values.

5.4. Alternative hypotheses for animal movement

Ungulate movements on the Pleistocene south coast of the GCFR could have operated in a number of ways. Our study was designed to test the Paleo-Agulhas Plain migration ecosystem hypothesis, which posits an eastern-summer to western-winter movement pattern, and an alternative hypothesis that ungulates moved between the interior and the coast. The Outeniqua Mountains separating the inter-montane basin (the Little Karoo) from the coastal plains are not particularly high (no more than 1400 m above sea level) and do have passes, so such a migration pattern is possible. Some historical accounts suggest that north to south animal movements occurred among elephants (Skead, 2011). The strontium isotope analysis of fossil teeth, as informed by the bioavailable strontium isoscape, has the potential to falsify the east-west migration hypothesis and test the north-south hypothesis. If the serial measurements showed large changes in $^{87}Sr/^{86}Sr$ from high values to low values, this would be supportive of a north-south movement and unsupportive of an east-west movement. The results of fossil teeth $^{87}Sr/^{86}Sr$ cannot falsify the east-west migration hypothesis, but do falsify a hypothesis of north-south movement. The evidence that ungulates did not move north of the Outeniqua Mountains suggests that the Pleistocene grazing ungulate communities of the intermontane basin (the Little Karoo) documented at sites such as Boomplaas (Faith, 2013), and those on the south coast sampled by PP30 and PP13B (Rector and Reed, 2010) were separate populations.

An alternative hypothesis is that ungulates in this region spent a significant amount of time on the foothills and dissected coastal plain south of the Outeniqua Mountains and north of the now-submerged Paleo-Agulhas Plain, and in general moved about the landscape utilizing patchy high quality graze, such as that in Renosterveld, in patches of nutrient-rich Bokkeveld Group shale sediments in the dissected plain (Radloff et al., 2010). In this scenario, we would expect strontium isotope ratios that are higher than those of bioavailable $^{87}Sr/^{86}Sr$ from the Bredasdorp Group and other areas immediately along the modern coast. The Bokkeveld Group shales appear to produce relatively high $^{87}Sr/^{86}Sr$ ratios that are overwhelmed by the abundance of marine-derived strontium (lower$^{87}Sr/^{86}Sr$) in the biosphere near the coast (Figure S2). Bokkeveld shales more than 30 km north of the modern coast have bioavailable $^{87}Sr/^{86}Sr$ greater than 0.712, while those from the interior can be higher than 0.720 (Table S2). The $^{87}Sr/^{86}Sr$ ratios in the fossils (0.709–0.711) are lower than would be expected if animals spent much time on Bokkeveld/Renosterveld, unless it was in patches near the coast or on exposed Cretaceous shales along the northern Paleo-Agulhas Plain. Comparison to the Sr isoscape model shows that the region of similar bioavailable Sr values to the fossils occurs predominantly on the exposed Paleo-Agulhas Plain and within the region ~15 km inland on the coastal plain. Thus, the strontium pattern measured in the fossils is most consistent with the ungulates spending the majority of their lives on marine-derived or seawater influenced sediments on or within about 15 km of the Paleo-Agulhas Plain.

Flowing south from the intermontane basin (Little Karoo) and dissected plain are several drainages that cut through Bokkeveld Group shales on their way to the south coast. During times of lower sea level, as they drained onto the flat Paleo-Agulhas Plain, they may have spread the nutrient-rich alluvium in north-south running strips (Marean et al., 2014). These would be high quality grazing areas favored by ungulates. Bokkeveld-/nutrient-rich soils have higher $^{87}Sr/^{86}Sr$ ratios than the Bredasdorp or other marine-derived sediments but can be swamped by marine-derived strontium. The relatively low $^{87}Sr/^{86}Sr$ ratios of the fossil teeth suggest that these alluvium locations were not present, or that they were not significantly grazed by the sampled ungulates. Alternatively, the Bokkeveld-/nutrient-rich soils might have been present, but contributed little strontium to the biosphere compared to marine-derived sea-spray, precipitation, and sediments on the relatively flat Paleo-Agulhas Plain. Offshore geophysical studies favor the explanation whereby such floodplain deposits were rapidly overlain, at least partially, by marine sediments such as sand dunes (Cawthra, 2014). This would add marine-derived strontium resulting in bioavailable $^{87}Sr/^{86}Sr$ ratios closer to 0.7092.

6. Conclusions

We created a bioavailable $^{87}Sr/^{86}Sr$ isoscape for the south coast of the GCFR region by analyzing plants from 171 sampling sites and developing a geospatial model. This provided a robust isoscape for interpreting the movement patterns of fossil ungulates dating to the Middle and Late Pleistocene from Pinnacle Point. Results indicate that ungulates did not spend significant amounts of time foraging on mountain, foothill, or dissected plain localities more than about 15 km north of the modern coastline. The results clearly exclude a north-south, interior-coastal movement or migration pattern. The strontium isotope evidence shows that these fossil ungulates foraged primarily on the now-submerged Paleo-Agulhas Plain habitats rather than those north of the modern coast line. This suggests that the open-habitat fauna that dominate the Pleistocene assemblages on the south coast derive from a population of animals largely restricted to the now-submerged Paleo-Agulhas Plain. Given this specialized use of this plain, this animal community would have suffered catastrophic habitat loss when sea levels rose during the Holocene and MIS 5e. Since bioavailable strontium varies from north to south but not from east to west, other isotope systems such as carbon and oxygen may be better suited for testing east-west movements based on fossil tooth enamel.

Acknowledgements

We would like to thank Jan Vlok for botanical expertise and help with sample collections, Kerryn Gray, Fayrooza Rawoort, and Hope Williams for help with laboratory analyses, John Lanham, Ian Newton, and Judith Sealy for support at the UCT Department of Archaeology stable isotope laboratory, and Paul Sandberg and Matt Sponheimer for helpful discussions. We would like to thank the anonymous reviewers, whose comments helped us to improve the manuscript. This research was funded by the National Science Foundation (# BCS-9912465, BCS-0130713, BCS-0524087, and BCS-1138073), the Hyde Family Foundations, the John Templeton Foundation, and the Institute of Human Origins (IHO) at Arizona State University. The opinions expressed in this publication are those of the author(s) and do not necessarily reflect the views of any of the granting agencies.

Appendix A. Supplementary data

Supplementary data related to this article can be found at http://dx.doi.org/10.1016/j.quascirev.2016.04.002.

References

Allsopp, H.L., Kolbe, P., 1965. Isotopic age determinations on the Cape granite and intruded Malmesbury sediments, Cape Peninsula, South Africa. Geochim. Cosmochim. Acta 29, 1115–1130.

Allsopp, N., Colville, J.F., Verboom, A.G. (Eds.), 2014. Fynbos: Ecology, Evolution and Conservation of a Megadiverse Region. Oxford University Press, Oxford.

Backeberg, N.R., Reid, D.L., Trumbull, R.B., Romer, R.L., 2011. Petrogenesis of the False Bay Dyke Swarm, Cape Peninsula, South Africa: evidence for basement assimilation. South Afr. J. Geol. 114, 335–352. http://dx.doi.org/10.2113/gssajg.114.3-4.335.

Balasse, M., 2002. Reconstructing dietary and environmental history from enamel isotopic analysis: time resolution of intra-tooth sequential sampling. Int. J. Osteoarchaeol. 12, 155–165.

Balasse, M., Ambrose, S.H., Smith, A., Price, T.D., 2002. The seasonal mobility model for prehistoric herders in the south-western Cape of South Africa assessed by isotopic analysis of sheep tooth enamel. J. Archaeol. Sci. 29, 917–932.

Bar-Matthews, M., Marean, C.W., Jacobs, Z., Karkanas, P., Fisher, E.C., Herries, A.I.R., Brown, K., Williams, H.M., Bernatchez, J., Ayalon, A., Nilssen, P.J., 2010. A high resolution and continuous isotopic speleothem record of paleoclimate and paleoenvironment from 90 to 53 ka from Pinnacle Point on the south coast of South Africa. Quat. Sci. Rev. 29, 2131–2145. http://dx.doi.org/10.1016/j.quascirev.2010.05.009.

Bataille, C.P., Laffoon, J., Bowen, G.J., 2012. Mapping multiple source effects on the strontium isotopic signatures of ecosystems from the circum-Caribbean region. Ecosphere 3, 1–24.

Bergh, N.G., et al., 2014. Vegetation types of the Greater Cape Floristic Region. In: Allsopp, N., Colville, J.F., Verboom, T. (Eds.), Fynbos: Ecology, Evolution, and Conservation of a Megadiverse Region. Oxford University Press, Oxford, pp. 1–25.

Blum, J., Taliaferro, E., Weisse, M., Holmes, R., 2000. Changes in Sr/Ca, Ba/Ca and 87Sr/86Sr ratios between trophic levels in two forest ecosystems in the northeastern USA. Biogeochemistry 49, 87–101.

Boshoff, A.F., Kerley, G., 2001. Potential distributions of the medium- to large-sized mammals in the Cape Floristic Region, based on historical accounts and habitat requirements. Afr. Zool. 36, 245–273.

Boshoff, A.F., Kerley, G.I.H., Cowling, R.M., 2001. A pragmatic approach to estimating the distributions and spatial requirements of the medium- to large-sized mammals in the Cape Floristic Region, South Africa. Divers. Distrib. 7, 29–43. http://dx.doi.org/10.1046/j.1472-4642.2001.00095.x.

Bradshaw, P.L., Cowling, R.M., 2014. Landscapes, rock types, and climate of the Greater Cape Floristic Region. In: Allsopp, N., Colville, J.F., Verboom, A.G. (Eds.), Fynbos: Ecology, Evolution and Conservation of a Megadiverse Region. Oxford University Press, Oxford, pp. 26–46.

Britton, K., Grimes, V., Dau, J., Richards, M.P., 2009. Reconstructing faunal migrations using intra-tooth sampling and strontium and oxygen isotope analyses: a case study of modern caribou (*Rangifer tarandus granti*). J. Archaeol. Sci. 36, 1163–1172. http://dx.doi.org/10.1016/j.jas.2009.01.003.

Britton, K., Grimes, V., Niven, L., Steele, T.E., McPherron, S., Soressi, M., Kelly, T.E., Jaubert, J., Hublin, J.-J., Richards, M.P., 2011. Strontium isotope evidence for migration in late Pleistocene Rangifer: implications for Neanderthal hunting strategies at the Middle Palaeolithic site of Jonzac, France. J. Hum. Evol. 61, 176–185. http://dx.doi.org/10.1016/j.jhevol.2011.03.004.

Broad, D.S., Jungslager, E.H.A., McLachlan, I.R., Roux, J., 2006. Offshore Mesozoic basins. In: Johnson, M.R., Annhauser, C.R., Thomas, R.J. (Eds.), The Geology of South Africa. Geological Society of South Africa. Johannesburg/Council for Geoscience, Pretoria, pp. 553–571.

Brown, W.A.B., Christofferson, P.V., Massler, M., Weiss, M.B., 1960. Postnatal tooth development in cattle. Am. J. Vet. Res. 21, 7e34.

Brown, K.S., Marean, C.W., Herries, A., Jacobs, Z., 2009. Fire as an engineering tool of early modern humans. Science 325, 859–862. http://dx.doi.org/10.1126/science.1175028.

Brown, K.S., Marean, C.W., Jacobs, Z., Schoville, B.J., Oestmo, S., Fisher, E.C., Bernatchez, J., Karkanas, P., Matthews, T., 2012. An early and enduring advanced technology originating 71,000 years ago in South Africa. Nature 491, 590. http://dx.doi.org/10.1038/nature11660.

Bryant, R.G., Bigg, G.R., Mahowald, N.M., Eckardt, F.D., Ross, S.G., 2007. Dust emission response to climate in southern Africa. J. Geophys. Res. Atmos. 112 http://dx.doi.org/10.1029/2005JD007025.

Budd, P., Montgomery, J., Barreiro, B., Thomas, R., 2000. Differential diagenesis of strontium in archaeological human dental tissues. Appl. Geochem. 15, 687–694.

Cawthra, H.C., 2014. The Marine Geology of Mossel Bay. PhD thesis. University of Cape Town, South Africa, 283 pp.

Cawthra, H.C., Bateman, M.D., Carr, A.S., Compton, J.S., Holmes, P.J., 2014. Understanding Late Quaternary change at the land–ocean interface: a synthesis of the evolution of the Wilderness coastline, South Africa. Quat. Sci. Rev. 99 (1), 210–223.

Cawthra, H.C., Compton, J.S., Fisher, E.C., Marean, C.W., 2015. Submerged shorelines and landscape features offshore of Mossel Bay, South Africa. In: Harff, J., Bailey, G., Lüth, F. (Eds.), Geology and Archaeology: Submerged Landscapes of the Continental Shelf, Special Publication of the Geological Society of London, vol. 411, pp. 219–233. http://dx.doi.org/10.1144/SP411.11.

Chadwick, O.A., Derry, L.A., Bern, C.R., Vitousek, P.M., 2009. Changing sources of strontium to soils and ecosystems across the Hawaiian Islands. Chem. Geol. 267, 64–76. http://dx.doi.org/10.1016/j.chemgeo.2009.01.009.
Chase, B.M., Meadows, M.E., 2007. Late Quaternary dynamics of southern Africa's winter rainfall zone. Earth-Sci. Rev. 84, 103–138. http://dx.doi.org/10.1016/j.earscirev.2007.06.002.
Chesson, L.A., Tipple, B.J., Mackey, G.N., Hynek, S.A., Fernandez, D.P., Ehleringer, J.R., 2012. Strontium isotopes in tap water from the coterminous USA. Ecosphere 3. http://dx.doi.org/10.1890/ES12-00122.1 art67.
Chiaradia, M., Gallay, A., Todt, W., 2003. Different contamination styles of prehistoric human teeth at a Swiss necropolis (Sion, Valais) inferred from lead and strontium isotopes. Appl. Geochem. 18, 353–370.
Clark, J.D., Beyene, Y., WoldeGabriel, G., Hart, W.K., Renne, P.R., Gilbert, H., Defleur, A., Suwa, G., Katoh, S., Ludwig, K.R., Boisserie, J.-R., Asfaw, B., White, T.D., 2003. Stratigraphic, chronological and behavioural contexts of Pleistocene Homo sapiens from Middle Awash, Ethiopia. Nature 423, 747–752. http://dx.doi.org/10.1038/nature01670.
Compton, J.S., 2011. Pleistocene sea-level fluctuations and human evolution on the southern coastal plain of South Africa. Quat. Sci. Rev. 30, 506–527. http://dx.doi.org/10.1016/j.quascirev.2010.12.012.
Copeland, S., Sponheimer, M., de Ruiter, D.J., Lee-Thorp, J.A., Codron, D., le Roux, P.J., Grimes, V., Richards, M.P., 2011. Strontium isotope evidence for landscape use by early hominins. Nature 474, 76–78. http://dx.doi.org/10.1038/nature10149.
Copeland, S., Sponheimer, M., Lee-Thorp, J.A., le Roux, P.J., de Ruiter, D.J., Richards, M.P., 2010. Strontium isotope ratios in fossil teeth from South Africa: assessing laser ablation MC-ICP-MS analysis and the extent of diagenesis. J. Archaeol. Sci. 37, 1437–1446. http://dx.doi.org/10.1038/j.jas.2010.01.003.
Cowling, R.M., 1983. The occurrence of C3 and C4 grasses in fynbos and allied shrublands in the South Eastern Cape, South Africa. Oecologia 58, 121–127. http://dx.doi.org/10.1007/BF00384551.
Cowling, R.M., Lombard, A.T., 2002. Heterogeneity, speciation/extinction history and climate: explaining regional plant diversity patterns in the Cape Floristic Region. Divers. Distrib. 8, 163–179.
Cowling, R.M., Potts, A.J., 2015. Climatic, edaphic and fire regime determinants of biome boundaries in the eastern Cape Floristic Region. South Afr. J. Bot. http://dx.doi.org/10.1016/j.sajb.2015.03.182.
Cowling, R.M., Proches, S., Partridge, T.C., 2009. Explaining the uniqueness of the Cape flora: incorporating geomorphic evolution as a factor for explaining its diversification. Mol. Phylogenet. Evol. 51, 64–74.
Cronwright-Schreiner, S.C., 1925. The Migratory Springbucks of South Africa. T. Fisher Unwin Ltd, London.
Culkin, F., Cox, R.A., 1966. Sodium, potassium, magnesium, calcium and strontium in sea water. Deep Sea Res. Oceanogr. Abstr. 13, 789–804. http://dx.doi.org/10.1016/0011-7471(76)90905-0.
de Villiers, S., Compton, J.S., Lavelle, M., 2000. The strontium isotope systematics of the Orange river, Southern Africa. South Afr. J. Geol. 103, 237–248.
Dingle, R.V., Siesser, W.G., Newton, A.R., 1983. Mesozoic and Tertiary Geology of Southern Africa, 375 ed. Balkema, Rotterdam.
Durante, C., Baschieri, C., Bertacchini, L., Cocchi, M., Sighinolfi, S., Silvestri, M., Marchetti, A., 2013. Geographical traceability based on Sr-87/Sr-86 indicator: a first approach for PDO Lambrusco wines from Modena. Food Chem. 141, 2779–2787. http://dx.doi.org/10.1016/j.foodchem.2013.05.108.
Ericson, J.E., 1985. Strontium isotope characterization in the study of prehistoric human ecology. J. Hum. Evol. 14, 503–514. http://dx.doi.org/10.1016/S0047-2484(85)80029-4.
Estes, R.D., 1991. The Behavior Guide to African Mammals. University of California Press, Berkeley.
Evans, J.A., Montgomery, J., Wildman, G., 2009. Isotope domain mapping of 87Sr/86Sr biosphere variation on the Isle of Skye, Scotland. J. Geol. Soc. 166, 617–631. http://dx.doi.org/10.1144/0016-76492008-043.
Evans, J.A., Montgomery, J., Wildman, G., Boulton, N., 2010. Spatial variations in biosphere 87Sr/86Sr in Britain. J. Geol. Soc. 167, 1–4. http://dx.doi.org/10.1144/0016-76492009-090.
Faith, J.T., 2013. Taphonomic and paleoecological change in the large mammal sequence from Boomplaas Cave, western Cape, South Africa. J. Hum. Evol. 65, 715–730. http://dx.doi.org/10.1016/j.jhevol.2013.09.001.
Faith, J.T., Thompson, J.C., 2013. Fossil evidence for seasonal calving and migration of extinct blue antelope (Hippotragus leucophaeus) in southern Africa. J. Biogeogr. 40, 2108–2118. http://dx.doi.org/10.1111/jbi.12154.
Fenner, J.N., Wright, L.E., 2014. Revisiting the strontium contribution of sea salt in the human diet. J. Archaeol. Sci. 44, 99–103. http://dx.doi.org/10.1016/j.jas.2014.01.020.
Fisher, E.C., Bar-Matthews, M., Jerardino, A., Marean, C.W., 2010. Middle and Late Pleistocene paleoscape modeling along the southern coast of South Africa. Quat. Sci. Rev. 29, 1382–1398. http://dx.doi.org/10.1016/j.quascirev.2010.01.015.
Franklin, J., Potts, A.J., Fisher, E.C., Cowling, R.M., Marean, C.W., 2015. Paleodistribution modeling in archaeology and paleoanthropology. Quat. Sci. Rev. 110, 1–14. http://dx.doi.org/10.1016/j.quascirev.2014.12.015.
Gadbury, C., Todd, L., Jahren, A.H., Amundson, R., 2000. Spatial and temporal variations in the isotopic composition of bison tooth enamel from the early Holocene Hudson–Meng Bone Bed, Nebraska. Palaeogeogr. Palaeoclimatol. Palaeoecol. 157, 79–93. http://dx.doi.org/10.1016/S0031-0182(99)00151-0.
Gage, J.P., Francis, M.J.O., Triffit, J.T., 1989. Collagen and Dental Matrices. Butterworth-Heinemann, London.
Goldblatt, P., Manning, J.C., 2002. Plant diversity of the Cape region of southern Africa. Ann. Mo. Botan. Gard. 281–302.
Gonder, M.K., Mortensen, H.M., Reed, F.A., de Sousa, A., Tishkoff, S.A., 2007. Whole-mtDNA genome sequence analysis of ancient African lineages. Mol. Biol. Evol. 24, 757–768.
Hälbich, I.W., 1983. A geodynamic model for the Cape Fold belt. In: Söhnge, A.P.G., Hälbich, I.W. (Eds.), Geodynamics of the Cape Fold Belt Special Publication of the Geological Society of South Africa, vol. 12, pp. 177–184.
Hartman, G., Richards, M., 2014. Mapping and defining sources of variability in bioavailable strontium isotope ratios in the Eastern Mediterranean. Geochim. Cosmochim. Acta 126, 250–264. http://dx.doi.org/10.1016/j.gca.2013.11.015.
Henn, B.M., Gignoux, C.R., Jobin, M., Granka, J.M., Macpherson, J.M., Kidd, J.M., Rodriguez-Botigue, L., Ramachandran, S., Hon, L., Brisbin, A., Lin, A.A., Underhill, P.A., Comas, D., Kidd, K.K., Norman, P.J., Parham, P., Bustamante, C.D., Mountain, J.L., Feldman, M.W., 2011. Hunter-gatherer genomic diversity suggests a southern African origin for modern humans. Proc. Natl. Acad. Sci. U. S. A. 108, 5154–5162. http://dx.doi.org/10.1073/pnas.1017511108.
Hoppe, K., Koch, P., 2007. Reconstructing the migration patterns of late Pleistocene mammals from northern Florida, USA. Quat. Res. 68, 347–352.
Hoppe, K., Koch, P., Furutani, T., 2003. Assessing the preservation of biogenic strontium in fossil bones and tooth enamel. Int. J. Osteoarchaeol. 13, 20–28.
Hoppe, K.A., Stover, S.M., Pascoe, J.R., Amundson, R., 2004. Tooth enamel biomineralization in extant horses: implications for isotopic microsampling. Palaeogeogr. Palaeoclimatol. Palaeoecol. 206, 355–365. http://dx.doi.org/10.1016/j.palaeo.2004.01.012.
Horne, R.A., 1969. Marine Chemistry; the Structure of Water and the Chemistry of the Hydrosphere. Wiley-Interscience.
Jacobs, Z., 2010. An OSL chronology for the sedimentary deposits from Pinnacle Point Cave 13B–A punctuated presence. J. Hum. Evol. 59, 289–305.
Janney, P.E., Roex, A.P.L., Carlson, R.W., Viljoen, K.S., 2002. A chemical and multi-isotope study of the Western Cape Olivine Melilitite Province, South Africa: implications for the sources of Kimberlites and the origin of the HIMU signature in Africa. J. Petrol. 43, 2339–2370. http://dx.doi.org/10.1093/petrology/43.12.2339.
Johnson, H.D., Baldwin, C.T., 1986. Shallow siliciclastic seas. In: Reading, H.G. (Ed.), Sedimentary Environments and Facies, second ed. Blackwell Scientific Publications, Oxford, pp. 229–282.
Johnson, M.R., van Vuuren, C.J., Visser, J.N.J., Cole, D.I., Wickens, de V., Christie, A.D.M., Roberts, D.L., Brandl, G., 2006. Sedimentary rocks of the Karoo Supergroup. In: Johnson, M.R., Annhauser, C.R., Thomas, R.J. (Eds.), The Geology of South Africa. Geological Society of South Africa/Council for Geoscience, Pretoria, pp. 461–501.
Julien, M.-A., Bocherens, H., Burke, A., Drucker, D.G., Patou-Mathis, M., Krotova, O., Péan, S., 2012. Were European steppe bison migratory? 18O, 13C and Sr intratooth isotopic variations applied to a palaeoethological reconstruction. Quat. Int. 271, 106–119. http://dx.doi.org/10.1016/j.quaint.2012.06.011.
Karkanas, P., Goldberg, P., 2010. Site formation processes at Pinnacle point Cave 13B (Mossel Bay, Western Cape Province, South Africa): resolving stratigraphic and depositional complexities with micromorphology. J. Hum. Evol. 59, 256–273. http://dx.doi.org/10.1016/j.jhevol.2010.07.001.
Kelly, R.L., 1995. The Foraging Spectrum. Smithsonian Institution Press, Washington D.C.
Klein, R.G., 1994. The long-horned African buffalo (Pelorovis antiquus) is an extinct species. J. Archaeol. Sci. 21, 725–733. http://dx.doi.org/10.1006/jasc.1994.1072.
Klein, R.G., 1983. Palaeoenvironmental implications of Quaternary large mammals in the Fynbos Region. In: Deacon, H.J., Hendey, Q.B., Lambrechts, J.J.N. (Eds.), Fynbos Palaeoecology: a Preliminary Synthesis. Cooperative Scientific Programmes, Pretoria, pp. 116–138.
Lee-Thorp, J., Sponheimer, M., 2003. Three case studies used to reassess the reliability of fossil bone and enamel isotope signals for paleodietary studies. J. Anthropol. Archaeol. 22, 208–216.
Lutjeharms, J.R.E., 2006. The Agulhas Current. Springer-Verlag, New York.
Lutjeharms, J.R.E., Monteiro, P.M.S., Tyson, P.D., Obura, D., 2001. The oceans around southern Africa and regional effects of global change. South Afr. J. Sci. 97, 119–130.
Malan, J.A., 1990. The Stratigraphy and Sedimentology of the Bredasdorp Group, Southern Cape Province. University of Cape Town.
Marean, C.W., 2014. The origins and significance of coastal resource use in Africa and Western Eurasia. J. Hum. Evol. 77, 17–40. http://dx.doi.org/10.1016/j.jhevol.2014.02.025.
Marean, C.W., 2011. Coastal South Africa and the co-evolution of the modern human lineage and coastal adaptations. In: Bicho, N., Haws, J.A., Davis, L.G. (Eds.), Trekking the Shore: Changing Coastlines and the Antiquity of Coastal Settlement. Springer, New York, pp. 421–440.
Marean, C.W., 2010. Pinnacle point cave 13B (Western Cape Province, South Africa) in context: the Cape Floral kingdom, shellfish, and modern human origins. J. Hum. Evol. 59, 425–443. http://dx.doi.org/10.1016/j.jhevol.2010.07.011.
Marean, C.W., Anderson, R.J., Bar-Matthews, M., Braun, K., Cawthra, H.C., Cowling, R.M., Engelbrecht, F., Esler, K.J., Fisher, E., Franklin, J., Hill, K., Janssen, M., Potts, A.J., Zahn, R., 2015. A new research strategy for integrating studies of paleoclimate, paleoenvironment, and paleoanthropology. Evol. Anthropol. 24, 62–72. http://dx.doi.org/10.1002/evan.21443.
Marean, C.W., Bar-Matthews, M., Bernatchez, J., Fisher, E., Goldberg, P., Herries, A.I.R., Jacobs, Z., Jerardino, A., Karkanas, P., Minichillo, T., Nilssen, P.J., Thompson, E., Watts, I., Williams, H.M., 2007. Early human use of marine resources and pigment in South Africa during the Middle Pleistocene. Nature 449,

905–908. http://dx.doi.org/10.1038/nature06204.
Marean, C.W., Bar-Matthews, M., Fisher, E., Goldberg, P., Herries, A., Karkanas, P., Nilssen, P.J., Thompson, E., 2010. The stratigraphy of the Middle Stone Age sediments at Pinnacle point cave 13B (Mossel Bay, Western Cape Province, South Africa). J. Hum. Evol. 59, 234–255. http://dx.doi.org/10.1016/j.jhevol.2010.07.007.
Marean, C.W., Cawthra, H.C., Cowling, R.M., 2014. Stone age people in a changing South African greater Cape Floristic Region. In: Allsopp, N., Colville, J.F., Verboom, T. (Eds.), Fynbos. Ecology, Evolution, and Conservation of a Mega-diverse Region, Ecology, Evolution, and Conservation of a Megadiverse Region. Oxford University Press, pp. 164–199. http://dx.doi.org/10.1093/acprof:oso/9780199679584.003.0008.
Marlowe, F.W., 2005. Hunter-gatherers and human evolution. Evol. Anthropol. 14, 54–67. http://dx.doi.org/10.1002/evan.20046.
Martin, A.K., Flemming, B.W., 1986. The Holocene shelf sediment wedge off the south and east coast of South Africa. In: Knight, R.J., McLean, J.R. (Eds.), Shelf Sands and Sandstones, Canadian Society of Petroleum Geologists Memoir, 2, pp. 27–44.
Martin, A.K., Hartnady, C.J.H., 1986. Plate tectonic development of the southeast Indian Ocean: a revised reconstruction of East Antarctica and Africa. J. Geophyis. Res. 91, 4767–4786.
Maurer, A.-F., Galer, S.J.G., Knipper, C., Beierlein, L., Nunn, E.V., Peters, D., Tütken, T., Alt, K.W., Schöne, B.R., 2012. Bioavailable 87Sr/86Sr in different environmental samples — Effects of anthropogenic contamination and implications for isoscapes in past migration studies. Sci. Total Environ. 433, 216–229. http://dx.doi.org/10.1016/j.scitotenv.2012.06.046.
McDougall, I., Brown, F.H., Fleagle, J.G., 2005. Stratigraphic placement and age of modern humans from Kibish, Ethiopia. Nature 433, 733–736.
Midgley, J.J., Harris, C., Harington, A., Potts, A.J., 2012. Geochemical perspective on origins and consequences of heuweltjie formation in the Southwestern Cape, South Africa. South Afr. J. Geol. 115, 577–588. http://dx.doi.org/10.2113/gssajg.115.4.
Milani, E.J., de Wit, M.J., 2008. Correlations between classic Parana and Cape-Karoo basins of South America and southern Africa and their basin infills flanking the Gondwanides: Du Toit revisited. In: Pankhurst, R.J., Trouw, R.A.J., de Brito Neves, B.B., de Wit, M.J. (Eds.), West Gondwana: Pre-Cenozoic Correlations across the South Atlantic Region, Geological Society, London, Special Publication, 294, pp. 319–342.
Mills, M.G.L., 1990. Kalahari Hyaenas: the Comparative Behavioural Ecology of Two Species. Unwin Hyman, London.
Montgomery, J., 2010. Passports from the past: investigating human dispersals using strontium isotope analysis of tooth enamel. Ann. Hum. Biol. 37, 325–346. http://dx.doi.org/10.3109/03014461003649297.
Montgomery, J., Evans, J.A., Horstwood, M.S.A., 2010. Evidence for long-term averaging of strontium in bovine enamel using TIMS and LA-MC-ICP-MS strontium isotope intra-molar profiles. Environ. Archaeol. 15, 32–42. http://dx.doi.org/10.1179/146141010X12640787648694.
Montgomery, J., Evans, J.A., Wildman, G., 2006. Sr-87/Sr-86 isotope composition of bottled British mineral waters for environmental and forensic purposes. Appl. Geochem. 21, 1626–1634. http://dx.doi.org/10.1016/j.apgeochem.2006.07.002.
Myers, N., Mittermeier, R.A., Mittermeier, C.G., da Fonseca, G.A.B., Kent, J., 2000. Biodiversity hotspots for conservation priorities. Nature 403, 853–858.
Newton, A.R., Shone, R.W., Booth, P.W.K., 2006. The Cape Fold Belt. In: Johnson, M.R., Annhauser, C.R., Thomas, R.J. (Eds.), The Geology of South Africa. Geological Society of South Africa. Johannesburg/Council for Geoscience Pretoria, pp. 521–531.
Odum, H.T., 1957. Strontium in Natural Waters. Publ. Inst. Mar. Sci. Univ, Texas IV (2).
Parker, R.J., Siesser, W.G., 1972. Petrology and origin of some phosphorites from the South African continental margin. J. Sediment. Res. 42, 434–440.
Paton, D.A., Macdonald, D.I.M., Underhill, J.R., 2006. Applicability of thin or thick skinned structural models in a region of multiple inversion episodes, southern. South Afr. J. Struct. Geol. 28, 1933–1947.
Passey, B., Cerling, T., 2002. Tooth enamel mineralization in ungulates: implications for recovering a primary isotopic time-series. Geochim. Cosmochim. Acta 66, 3225–3234.
Pellegrini, M., Donahue, R.E., Chenery, C., Evans, J., Lee-Thorp, J.A., Montgomery, J., Mussi, M., 2008. Faunal migration in late-glacial central Italy: implications for human resource exploitation. Rapid Comm. Mass Spectrom. 22, 1714–1726.
Petit, J.R., Jouzel, J., Raynaud, D., Barkov, N.I., Barnola, J.M., Basile, I., Bender, M., Chappellaz, J., Davis, M., Delaygue, G., Delmotte, M., Kotlyakov, V.M., Legrand, M., Lipenkov, V.Y., Lorius, C., Pepin, L., Ritz, C., Saltzman, E., Stievenard, M., 1999. Climate and atmospheric history of the past 420,000 years from the Vostok ice core, Antarctica. Nature 399, 429–436.
Pickrell, J.K., Patterson, N., Barbieri, C., Berthold, F., Gerlach, L., Guldemann, T., Kure, B., Mpoloka, S.W., Nakagawa, H., Naumann, C., Lipson, M., Loh, P.-R., Lachance, J., Mountain, J., Bustamante, C.D., Berger, B., Tishkoff, S.A., Henn, B.M., Stoneking, M., Reich, D., Pakendorf, B., 2012. The genetic prehistory of southern Africa. Nat. Commun. 3, 1143. http://dx.doi.org/10.1038/ncomms2140.
Pin, C., Briot, D., Bassin, C., Poitrasson, F., 1994. Concomitant separation of strontium and samarium-neodymium for isotopic analysis in silicate samples, based on specific extraction chromatography. Anal. Chim. Acta 298, 209–217.
Poszwa, A., Ferry, B., Pollie, B., Grimaldi, C., Charles-Dominique, P., Loubet, M., Dambrine, E., 2009. Variations of plant and Soil Sr-87/Sr-86 along the slope of a tropical inselberg. Ann. For. Sci. 66 http://dx.doi.org/10.1051/forest/2009036.
Price, T.D., Johnson, C., Ezzo, J., Burton, J., Ericson, J., 1994. Residential mobility in the prehistoric southwest United States: a preliminary study using strontium isotope analysis. J. Archaeol. Sci. 21, 315–315.
Price, T.D., Meiggs, D., Weber, M.J., Pike-Tay, A., 2015. The migration of Late Pleistocene reindeer: isotopic evidence from northern Europe. Archaeol. Anthropol. Sci. http://dx.doi.org/10.1007/s12520-015-0290-z.
Radloff, F., Mucina, L., Bond, W.J., Roux, P.J., 2010. Strontium isotope analyses of large herbivore habitat use in the Cape Fynbos region of South Africa. Oecologia 164, 567–578. http://dx.doi.org/10.1007/s00442-010-1731-0.
Rautenbach, I.L., 1971. Ageing criteria in the springbok, Antidorcas Marsupialis (Zimmermann, 1780) (Artiodactyla: Bovidae). Ann. Transvaal Mus. 27, 83–133.
Rector, A., Reed, K.E., 2010. Middle and late Pleistocene faunas of Pinnacle Point and their paleoecological implications. J. Hum. Evol. 59, 340–357. http://dx.doi.org/10.1016/j.jhevol.2010.07.002.
Roberts, D.L., Cawthra, H.C., Musekiwa, C., 2013. Dynamics of late Cenozoic aeolian deposition along the South African coast: a record of evolving climate and ecosystems. In: Martini, I.P., Wanless, H.R. (Eds.), Sedimentary Coastal Zones from High to Low Latitudes: Similarities and Differences, Geological Society, London, Special Publications, 388.
Rogers, J., 1971a. Quaternary sediments of the Agulhus bank, Cape point to Cape St. Francis. In: Sancor Technical Report No. 3. Department of Geology, University of Cape Town, Cape Town.
Rogers, J., 1971b. Sedimentology of Quaternary Deposits on the Agulhas Bank. University of Cape Town.
Rozendaal, A., Gresse, P.G., Scheepers, R., Le Roux, J.P., 1999. Neoproterozoic to early Cambrian crustal evolution of the Pan-African Saldania belt, South Africa. Precambrian Res. 97 (3–4), 303–323.
Schlebusch, C.M., Skoglund, P., Sjöin, P., Gattepaille, L.M., Hernandez, D., Jay, F., Li, S., De Jongh, M., Singleton, A., Blum, M.G.B., Soodyall, H., Jakobsson, M, 2012. Genomic variation in seven Khoe-San groups reveals adaptation and complex African history. Science 338, 374–379.
Schulze, B.R., 1972. South Africa. In: Griffiths, J.F. (Ed.), Climates of Africa, World Survey of Climatology, 10. Elsevier, Amsterdam, pp. 501–566.
Sealy, J., 1996. Seasonality of rainfall around the Last Glacial Maximum as reconstructed from carbon isotope analyses of animal bones from Nelson Bay Cave. South Afr. J. Sci. 92, 441–444.
Sealy, J., van der Merwe, N., Sillen, A., 1991. 87Sr/86Sr as a dietary indicator in modern and archaeological bone. J. Archaeol. Sci. 18, 399–416.
Sillen, A., Hall, G., Richardson, S., Armstrong, R., 1998. 87Sr/86Sr ratios in modern and fossil food-webs of the Sterkfontein Valley: implications for early hominid habitat preference. Geochim. Cosmochim. Acta 62, 2463–2473.
Skead, C.J., 2011. Historical Incidence of the Larger Land Mammals in the Broader Western and Northern Cape. Nelson Mandela Metropolitan University, Port Elizabeth.
Skinner, J.D., Smithers, R.H.N., 1990. The Mammals of the Southern African Subregion. University of Pretoria, Pretoria.
Soderberg, K., Compton, J.S., 2007. Dust as a nutrient source for fynbos ecosystems, South Africa. Ecosystems 10, 550–561. http://dx.doi.org/10.1007/s10021-007-9032-0.
Thamm, A.G., Johnson, M.R., 2006. The Cape Supergroup. In: Johnson, M.R., Annhauser, C.R., Thomas, R.J. (Eds.), The Geology of South Africa. Geological Society of South Africa, Johannesburg/Council for Geoscience, Pretoria, pp. 443–461.
Thompson, J.C., 2010. Taphonomic analysis of the Middle Stone Age faunal assemblage from Pinnacle point cave 13B, Western Cape, South Africa. J. Hum. Evol. 59, 321–339.
Thwaites, Cowling, 1988. Soil-vegetation relationships on the Agulhas plain, South Africa. Catena 15, 333–345.
Tinker, J.H., de Wit, M.J., Brown, R.W., 2008. Linking source and sink: evaluating the balance between onshore erosion and offshore sediment accumulation since Gondwana break-up, South Africa. Tectonophysics 455, 94–103.
Van Andel, T.H., 1989. Late Pleistocene sea levels and the human exploitation of the shore and shelf of southern South Africa. J. Field Archaeol. 16, 133–155.
Vickery, K.J., Eckardt, F.D., Bryant, R.G., 2013. A sub-basin scale dust plume source frequency inventory for southern Africa, 2005-2008. Geophys. Res. Lett. 40, 5274–5279. http://dx.doi.org/10.1002/grl.50968.
Vlok, J.H.J., Euston-Brown, D.I.W., Cowling, R.M., 2003. Acocks' Valley Bushveld 50 years on: new perspectives on the delimitation, characterization and origin of subtropical thicket vegetation. South Afr. J. Bot. 69, 27–51.
Voerkelius, S., Lorenz, G.D., Rummel, S., Quétel, C.R., Heiss, G., Baxter, M., Brach-Papa, C., Deters-Itzelsberger, P., Hoelzl, S., Hoogewerff, J., Ponzevera, E., Van Bocxstaele, M., Ueckermann, H., 2010. Strontium isotopic signatures of natural mineral waters, the reference to a simple geological map and its potential for authentication of food. Food Chem. 118, 933–940. http://dx.doi.org/10.1016/j.foodchem.2009.04.125.
Vogel, J.C., Fuls, A., Ellis, R.P., 1978. The geographical distribution of Kranz grasses in South Africa. South Afr. J. Sci. 74, 209–215.
Warham, J.O., 2011. Mapping Biosphere Strontium Isotope Ratios across Major Lithological Boundaries: a Systematic Investigation of the Major Influences on Geographic Variation in the 87Sr/86Sr Composition of Bioavailable Strontium above the Cretaceous and Jurassic Rocks of England. Ph.D. thesis. University of Bradford.
Watkeys, M.K., 2006. Gondwana break-up: a South African perspective. In: Johnson, M.R., Annhauser, C.R., Thomas, R.J. (Eds.), The Geology of South Africa. Geological Society of South Africa, Johannesburg/Council for Geoscience, Pretoria, pp. 531–539.

Whipkey, C., Capo, R., Chadwick, O., Stewart, B., 2000. The importance of sea spray to the cation budget of a coastal Hawaiian soil: a strontium isotope approach. Chem. Geol. 168, 37–48.

Zazzo, A., Balasse, M., 2005. High-resolution $\delta^{13}C$ intratooth profiles in bovine enamel: implications for mineralization pattern and isotopic attenuation. Geochim. Cosmochim. Acta 69, 3631–3642. http://dx.doi.org/10.1016/j.gca.2005.02.031.

Zazzo, A., Balasse, M., Passey, B., Moloney, A.P., Monahan, F.J., Schmidt, O., 2010. The isotope record of short- and long-term dietary changes in sheep tooth enamel: implications for quantitative reconstruction of paleodiets. Geochim. Cosmochim. Acta 74, 3571–3586.